

Synergy of exchange bias with superconductivity in ferromagnetic-superconducting layered hybrids: the influence of in-plane and out-of-plane magnetic order on superconductivity

D. Stamopoulos,* E. Manios, and M. Pissas

Institute of Materials Science, NCSR "Demokritos", 153-10, Aghia Paraskevi, Athens, Greece.

(Dated: February 2, 2008)

It is generally believed that superconductivity and magnetism are two antagonistic long-range phenomena. However, as it was preliminarily highlighted in D. Stamopoulos *et al.* [Phys. Rev. B **75**, 014501 (2007)] and extensively studied in this work under specific circumstances these phenomena instead of being detrimental to each other may even become cooperative so that their synergy may promote the superconducting properties of a hybrid structure.

Here, we have studied systematically the magnetic and transport behavior of such *exchange biased* hybrids that are comprised of ferromagnetic (FM) $\text{Ni}_{80}\text{Fe}_{20}$ and low- T_c superconducting (SC) Nb for the case where the magnetic field is applied *parallel* to the specimens. Two structures have been studied: FM-SC-FM trilayers (TLs) and FM-SC bilayers (BLs). Detailed magnetization data on the *longitudinal* and *transverse* magnetic components are presented for both the *normal* and *superconducting* states. These data are compared to systematic transport measurements including I-V characteristics. The comparison of the exchange biased BLs and TLs that are studied here with the plain ones studied in D. Stamopoulos *et al.* [Phys. Rev. B **75**, 184504 (2007)] enable us to reveal an underlying parameter that may falsify the interpretation of the transport properties of relevant FM-SC-FM TLs and FM-SC BLs investigated in the recent literature: the underlying mechanism motivating the extreme magnetoresistance peaks in the TLs relates to the suppression of superconductivity mainly due to the magnetic coupling of the two FM layers as the *out-of-plane* rotation of their magnetizations takes place across the coercive field where stray fields emerge in their whole surface owing to the multidomain magnetic state that they acquire. The relative *in-plane* magnetization configuration of the outer FM layers exerts a secondary contribution on the SC interlayer. Since the exchange bias directly controls the in-plane magnetic order it also controls the out-of-plane rotation of the FMs' magnetizations so that the magnetoresistance peaks may be tuned at will.

All the contradictory experimental data reported in the recent literature are fairly discussed under the light of our results; based on a specific prerequisite we propose a phenomenological stray-fields mechanism that explains efficiently the evolution of magnetoresistance effect in TLs. Our experiments not only point out the need for a new theoretical treatment of FM-SC hybrids but also direct us toward the design of efficient supercurrent-switch elemental devices.

PACS numbers: 74.45.+c, 74.78.Fk, 74.78.Db

I. INTRODUCTION

In recent years a new class of devices efficient for the control of current flow has emerged. Since unlikely to conventional electronics in this new class it is the electron's spin (than its charge degree of freedom) that is manipulated these devices are called spin valves. Various types of spin valves have been proposed. In all cases the basic core consists of a trilayer (TL) which hosts two ferromagnetic (FM) outer electrodes with an interlayer which can be either metallic,^{1,2,3} insulating^{4,5,6,7} or superconducting (SC).^{8,9,10,11,12,13,14,15,16,17,18,19}

The so-called superconducting spin valve was introduced theoretically in Refs.16,17. It is based on a FM-SC-FM TL where the nucleation of superconductivity can be manipulated by the relative in-plane magnetization orientation of the outer FM layers. Gu *et al.*⁸ were the first to report on the experimental realization of a $[\text{Ni}_{82}\text{Fe}_{18}\text{-Cu}_{0.47}\text{Ni}_{0.53}]/\text{Nb}/[\text{Cu}_{0.47}\text{Ni}_{0.53}\text{-Ni}_{82}\text{Fe}_{18}]$ spin valve. Soon after, Potenza *et al.*,⁹ and Moraru *et al.*^{10,11} confirmed the results that were re-

ported in Ref.8. In these works^{8,9,10,11} the exchange bias was employed in order to "pin" the magnetization of the one FM layer so that the relative magnetic configuration of the outer FM layers to be controlled. In agreement to the theoretical propositions^{16,17} it was observed^{8,9,10,11} that when the relative in-plane magnetization configuration of the two FM layers was parallel [antiparallel] the resistive transition of the SC was placed at lower [higher] temperatures. Peña *et al.*,¹² and Rusanov *et al.*¹³ have studied $\text{La}_{0.7}\text{Ca}_{0.3}\text{MnO}_3\text{-YBa}_2\text{Cu}_3\text{O}_7\text{-La}_{0.7}\text{Ca}_{0.3}\text{MnO}_3$ and $\text{Ni}_{80}\text{Fe}_{20}\text{-Nb-Ni}_{80}\text{Fe}_{20}$ TLs, respectively. Both works^{12,13} reported that the antiparallel in-plane magnetization configuration of the FM layers suppresses superconductivity when compared to the parallel one. Very recently, Visani *et al.*¹⁴ studied $\text{La}_{0.7}\text{Ca}_{0.3}\text{MnO}_3\text{-YBa}_2\text{Cu}_3\text{O}_7\text{-La}_{0.7}\text{Ca}_{0.3}\text{MnO}_3$ TLs and confirmed the results that were originally reported in Ref. 12. While the works mentioned above^{8,9,10,11,12,13,14} referred to the case where the magnetic field was applied parallel to the TLs (parallel-field configuration), Singh *et al.*¹⁵ reported on the case where it was applied nor-

mal to the specimens (normal-field configuration) for Co-Pt/Nb/Co-Pt TLs having perpendicular magnetic anisotropy and confirmed Refs.12,13,14. It should be stressed that in Refs.12,13,14,15 the exchange bias was *not* used for the control of the relative in-plane magnetic orientation of the two FM layers. Given that the results of Refs.8,9,10,11, where the exchange bias was employed, are the opposite to the ones of Refs.12,13,14,15, where this mechanism was *not* employed, it is natural to suppose that, except for the relative in-plane magnetization configuration of the outer FM layers, it is the presence of exchange bias that probably has influenced the properties of the SC interlayer altering drastically the experimental results obtained in Refs.8,9,10,11.

Indeed, detailed magnetization data that were presented in Refs.20,21,22 for the parallel-field configuration in hybrids constructed of multilayer (ML) $[\text{La}_{0.33}\text{Ca}_{0.67}\text{MnO}_3/\text{La}_{0.60}\text{Ca}_{0.40}\text{MnO}_3]_{15}$ and SC Nb revealed that the exchange bias mechanism clearly influences the SC's magnetic behavior. More specifically, the magnetization results presented in Refs.20,21 revealed an effective ferromagnetic coupling between the ML and the adjacent SC that in microscopic level was compatible with recent theoretical proposals on the formation of spin-triplet superconductivity that were presented in Refs.18,23,24,25,26,27 (see also Refs.28,29). Also, in Refs.21,22 it was shown that superconductivity was enhanced significantly when the ML was in a state of almost zero bulk magnetization where a multidomain configuration was acquired. The magnetization results of Refs.21,22 supported the recent theoretical proposals on the so-called "domain-wall superconductivity" of Refs.30,31,32,33,34,35,36,37 suggesting that when the superconducting pairs have the opportunity to sample different directions of the exchange field the imposed pair-breaking effect is only minimum. On the other hand, when these results are discussed in a macroscopic level apart from the exchange interaction also the electromagnetic mechanism^{36,37} related to the magnetic stray fields that enter the SC alongside the interface with the ML could motivate equally well the experimental effects observed in Refs.20,21,22. Indeed, very recently Monton et al.³⁸ studied Nb/Co MLs in the parallel-field configuration and reported a behavior similar to the one observed in Refs.20,21,22. These authors³⁸ interpreted their results based exclusively on the influence of the FMs' stray fields on the SC layers. However, that work³⁸ not only confirmed some of the observations that were originally reported in Refs.20,21,22 but expanded our knowledge to the complete mutual effect; the authors³⁸ revealed that the screening coming from the SC layers influences drastically the magnetic domain state of the adjacent FM ones.

Referring to the normal-field configuration Moshchalkov and colleagues revealed the importance of stray fields for the case of Co-Pd/Nb/Co-Pd TLs, $\text{BaFe}_{12}\text{O}_{19}$ -Nb BLs and $\text{PbFe}_{12}\text{O}_{19}$ -Nb BLs that were studied in Refs.39, 40 and 41, respectively. In

these works^{39,40,41} where an insulating interlayer was deposited between the SC and FM layers in order the electronic coupling to be removed, the spatial evolution of superconductivity nucleation above domain walls and inside magnetic domains was studied extensively. Also, for simple BLs we note that a magnetoresistance effect was observed by Ryazanov et al. in Ref.42 for the case of $\text{Nb-Cu}_{0.43}\text{Ni}_{0.57}$ hybrids. These authors attributed the magnetoresistance effect to the dissipation produced by the flow of vortices since the SC's lower critical field is exceeded by the FM's stray fields that emerge due to its multidomain magnetic structure attained at coercivity. Very recently, in Ref.43 Aarts and colleagues have concluded to the same interpretation for the pronounced magnetoresistance effect that they observed in all-amorphous GdNi-MoGe-GdNi TLs for the parallel-field configuration.

Steiner and Ziemann in Ref.44 have dealt with the parallel-field configuration in a variety of hybrid TLs and BLs consisting of Co, Fe and Nb by performing transport and *longitudinal* magnetization measurements. These authors also employed micromagnetic simulations to convincingly show that in their samples the stray fields that emerge at coercivity are related to the observed magnetoresistance peaks. However, the magnetization measurements that were presented in Ref.44 referred only to the *longitudinal* magnetic component and were limited in the *normal* state of the SC constituent.

Experimental data on both the *longitudinal* and *transverse* magnetic components that were obtained not only in the *normal* but also in the *superconducting* state were presented in our recent work, Ref.45 where we investigated these topics in relevant FM-SC-FM TLs and FM-SC BLs that were constructed of low spin polarized $\text{Ni}_{80}\text{Fe}_{20}$ and low- T_c Nb. While the detailed results that were presented in Ref.45 refer to plain TLs and BLs, the ones that were reported in Ref.46 relate to the respective specimens that incorporate the mechanism of exchange bias. The preliminary data that we reported in Ref.46 for exchange biased $\text{Ni}_{80}\text{Fe}_{20}$ -Nb- $\text{Ni}_{80}\text{Fe}_{20}$ TLs were in agreement [contrast] to the ones presented in Refs.12,13,14 [Refs.8,9,10,11] and showed evidence that the parallel [antiparallel] in-plane magnetization configuration of the outer FM layers promotes [suppresses] the transport properties of the SC interlayer. On the other hand, the detailed results that were presented in Ref.45 for plain $\text{Ni}_{80}\text{Fe}_{20}$ -Nb- $\text{Ni}_{80}\text{Fe}_{20}$ TLs revealed a pronounced dissipation peak that, although it was significantly stronger than the one reported by Rusanov et al. in Ref.13 for $\text{Ni}_{80}\text{Fe}_{20}$ -Nb- $\text{Ni}_{80}\text{Fe}_{20}$ TLs of robust uniaxial magnetic anisotropy, it was quantitatively identical to the one reported by Peña et al., in Ref.12 and Visani et al., in Ref.14 for the case of $\text{La}_{0.7}\text{Ca}_{0.3}\text{MnO}_3$ - $\text{YBa}_2\text{Cu}_3\text{O}_7$ - $\text{La}_{0.7}\text{Ca}_{0.3}\text{MnO}_3$ TLs. However, in Ref.45 we have attributed the pronounced dissipation peaks to a different underlying mechanism than the one reported in Refs.12,13,14. By performing measurements on the TLs' *transverse* magnetic component in both the nor-

mal and superconducting states, we clearly showed that below its T_c^{SC} the Nb interlayer under the influence of the outer NiFe layers attains a magnetization component *transverse* to the external magnetic field. When these *transverse* magnetization data were compared to the transport ones it was revealed that the pronounced magnetoresistance peaks that are observed in the low-field regime are due to the suppression of superconductivity by *transverse* stray fields that they interconnect the outer $\text{Ni}_{80}\text{Fe}_{20}$ layers. Long time ago relevant features were also observed in FM-IN-FM and FM-NM-FM TLs (where IN and NM stand for insulator and non magnetic metal, respectively). For instance, S. Parkin and colleagues^{4,47} have clearly shown that in such TLs of IN/NM interlayer the magnetostatic interaction of the outer FM layers through stray fields, that may be farther promoted by surface roughness,^{47,48,49} could lead to their significant overall magnetostatic coupling. This stray-fields coupling plays a unique role in FM-IN-FM and FM-NM-FM TLs since it alters drastically the distinct magnetic character of the outer FM layers; ultimately this mechanism makes a "magnetically hard" FM layer to rather behave as "magnetically soft". Except for the influence of surface roughness,^{47,48,49} the out-of-plane rotation of the magnetization and the subsequent magnetostatic coupling of the outer FM layers could be promoted or suppressed by other parameters such as (a) the intrinsic magnetic anisotropy of the specific FM materials, and (b) the extrinsic, shape-induced magnetic anisotropy that is related to the thickness of the employed FM layers. Returning to the case of our FM-SC-FM TLs we stress that since the only difference between the FM-SC hybrids studied in Refs.45 and 46 was the presence of exchange bias it was natural to examine whether the mechanism that was employed in Ref.45 for the interpretation of the experimental results obtained in plain TLs and BLs also holds for the exchange biased ones that were only preliminary highlighted in Ref.46.

This is the main topic of our current work: presenting detailed magnetization and transport results that uncover the underlying mechanism that motivates the relative promotion of superconductivity in exchange biased FM-SC hybrids as it was recently reported in Ref.46. We stress that in this work we study the parallel-field configuration as was done in all other Refs.8,9,10,11,12,13,14,44,45,46,50 so that a straightforward comparison may be rightfully performed. However, our proposals could be applicable to results that were obtained for the normal-field configuration that was studied in Refs.15,39,40,41,42. The presented magnetization data refer not only to the *longitudinal* magnetic component (parallel to the externally applied magnetic field) but also to the *transverse* one (normal to the externally applied magnetic field). Furthermore, we present data that are obtained not only in the *normal* regime of the SC but also in its *superconducting* state. Such data have not been presented in the literature and are shown here for the first time. In agreement to the results obtained in Ref.45 for

plain samples, here we clearly show that even in exchange biased ones the *transverse* magnetization data reveal crucial information for the interpretation of the effects that are observed in the magnetoresistance:

The extreme magnetoresistance peaks observed in the TLs are primarily [secondarily] motivated by the magnetic coupling of the outer FM layers as their magnetizations rotate out-of-plane [in-plane] at the coercive field. The formed transverse magnetization field that penetrates the SC interlayer ultimately suppresses its superconducting properties since it primarily [secondarily] exceeds its lower [upper] critical field. Referring to the BLs although out-of-plane rotation of the magnetization of the single FM layer is still observed, due to the absence of a second FM layer in these structures magnetic coupling doesn't occur so that the observed magnetoresistance peaks are only modest. Consequently, in FM-SC-FM TLs the relative in-plane magnetization configuration is not the only parameter that should be examined, as was done in Refs.8,9,10,11,12,13,14,46. *Primarily the out-of-plane magnetization configuration should be considered as the underlying mechanism of the pronounced magnetoresistance peaks.* This new experimental outcome assists us toward understanding the contradictory transport data that have been obtained recently in relevant FM-SC-FM TLs.^{8,9,10,11,12,13,14,46}

Most importantly, here we show that since the exchange bias mechanism directly controls the in-plane magnetic order it also controls the out-of-plane rotation of the FMs' magnetization so that the magnetoresistance peaks may be tailored at will. Uncontested evidence is presented through I-V characteristics for the virgin and exchange biased states of the hybrids that exchange bias relatively promotes the transport ability of the complete hybrid. Also, the so-called training effect that accompanies the exchange bias in the normal state is clearly preserved even in the superconducting state and controls the transport behavior of the SC.

Finally, a fair comparison of all the relevant experimental works that have treated both exchange biased and plain FM-SC-FM TLs and FM-SC BLs is carried out. Based on a prerequisite that should hold for the coercive fields of the outer FM layers we propose a plausible stray-fields mechanism that explains efficiently all the available experiments that were brought in our attention in the recent literature.

The present article is structured as following. Section II presents the sample preparation techniques and experimental details. Section III is devoted to the TL structures: subsection III.A presents detailed magnetic characterization in order to clearly reveal all the specific characteristics of the exchange bias mechanism in our samples, subsections III.B and III.C present comparatively transport and magnetization data for both the longitudinal and transverse components, and in subsection III.D we discuss the results obtained in our TLs and propose a stray-fields coupling mechanism that considering it is based on a specific requisite is also consistent

with other current experiments. Finally, in subsection III.E we show I-V characteristics for the TLs. Section IV refers to BLs and is divided in subsection IV.A which presents comparative transport and magnetization data, and in subsection IV.B which is exclusively devoted to the training effect that is observed in both the transport and magnetization data. Finally, section V summarizes our observations and presents the possible impact that these may have on current and future experimental and theoretical works.

II. PREPARATION OF SAMPLES AND EXPERIMENTAL DETAILS

The samples were sputtered on Si [001] substrates under an Ar environment (99.999% pure). In order to eliminate the residual oxygen that possibly existed in the chamber we performed Nb pre-sputtering for very long times.⁵¹ During the pre-sputtering process all the residual oxygen was absorbed by the dummy Nb. This procedure has a direct impact on the quality of the produced films.⁵¹ The Nb layers were deposited by dc-sputtering at 46 W and an Ar pressure of 3 mTorr. More details may be found in Ref.51. For the $\text{Ni}_{80}\text{Fe}_{20}$ (NiFe) layers rf-sputtering was employed at 30 W and 4 mTorr. We should stress that: (i) all depositions were carried out *at room temperature* and (ii) *no* magnetic field was applied during the deposition of the NiFe layers. However, the samples can't be shielded from the residual magnetic fields existing in the chamber of our magnetically-assisted-sputtering unit. Measurements by means of a Hall sensor revealed that at the place where the substrates are mounted the residual fields exhibit parallel components of magnitude 10–15 Oe at maximum. Thus, our NiFe films exhibit in-plane anisotropy. However, they don't exhibit detectable uniaxial anisotropy since the magnetic field sources are placed symmetrically on the perimeter of the circular rf-gun (for more details see the magnetization results presented in Ref.45). In order to inflict the mechanism of exchange bias^{52,53,54} the NiFe *bottom* layers were annealed systematically under O_2 (99.999% pure), Ar (99.999% pure) or reductive Ar-H_2 (94% – 6% mixture) atmosphere for durations in the range 2–24 hours at low temperatures 100–200 C. Afterwards, the complete BL or TL structures were deposited on top. As a result, in the exchange biased structures the NiFe bottom layer possesses exchange bias, while the top one (for the TLs) is always plain. In the rest of this work we will call: exchange biased TLs as BFM-SC-PFM, exchange biased BLs as BFM-SC, plain TLs as PFM-SC-PFM, and finally plain BLs as PFM-SC ("B" stands for "biased" and "P" for "plain"). The thicknesses are in the range 20 – 40 nm for the NiFe outer layers, while for Nb the thickness varies between 40 – 60 nm.

Our magnetoresistance measurements were performed by applying a dc-transport current (always normal to the magnetic field) and measuring the voltage in the standard

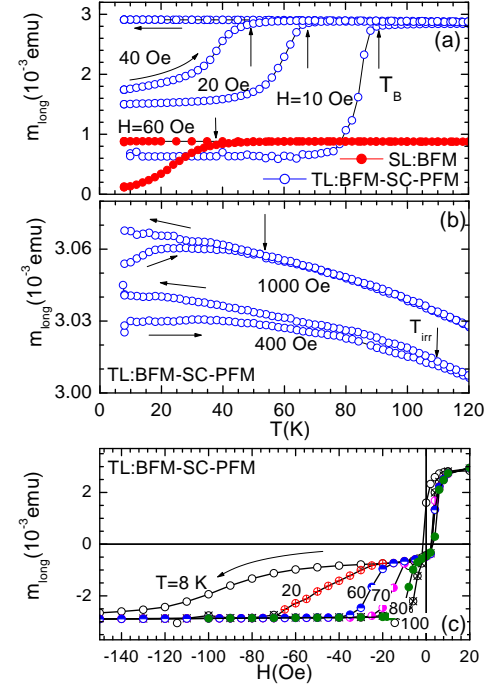


FIG. 1: (Colour online) Zero-field cooled and field cooled isofield $m(T)$ curves of the longitudinal component obtained in the temperature range $8 \text{ K} < T < 120 \text{ K}$ for a TL:BFM-SC-PFM (open circles) and a SL:BFM (solid circles) at relatively low (a) and high (b) values of the external magnetic field. (c) Isothermal loop measurements at various temperatures from above $T_B = 90 \text{ K}$ down to 8 K . For the sake of clarity only the decreasing branches are shown.

four-point configuration. In most of the measurements the applied current was $I_{\text{dc}} = 0.5 \text{ mA}$, which corresponds to an effective density $J_{\text{dc}} \approx 900 \text{ A/cm}^2$ (typical in plane dimensions of the films are $6 \times 5 \text{ mm}^2$). The temperature control and the application of the magnetic fields were achieved in a superconducting quantum interference device (SQUID) (Quantum Design). In all cases the applied field was *parallel* to the films.

III. EXCHANGE BIASED TLS

A. Magnetic characterization of the samples

The data presented in Figs. 1(a)-1(c) refer to the longitudinal magnetic component (parallel to the external magnetic field which in turn is applied parallel to the specimen's surface as it is schematically presented in the inset of Fig. 7, below). Such data are needed for a thorough magnetic characterization of the produced TLs. In panels (a) and (b) we show both the zero-field cooled and field cooled isofield $m_{\text{long}}(T)$ curves obtained in the temperature range $8 \text{ K} < T < 120 \text{ K}$ for a TL at relatively low and high values of the external magnetic field, respectively. In addition, we show one representative curve

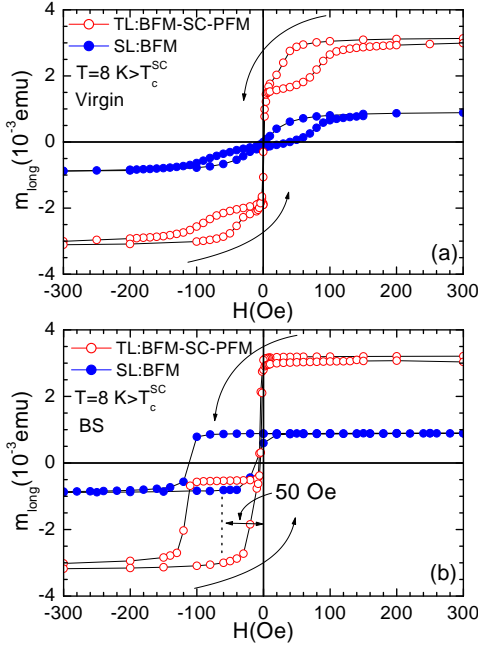


FIG. 2: (Colour online) Magnetization loops of the longitudinal component obtained at $T = 8$ K for a TL:BFM-SC-PFM (open circles) and a SL:BFM (solid circles) when the samples were virgin (a) and when exchange biased (b).

for a NiFe BFM single layer (SL) (solid circles) in order to stress that the behavior exhibited by the TL is exclusively related to its bottom BFM NiFe layer. We clearly see that a blocking temperature^{53,54} may be identified with $T_B = 90$ K for this particular TL. In all the TLs that have been studied the blocking temperature ranges between $90 \text{ K} < T_B < 100 \text{ K}$. As we see, above T_B even the lowest applied magnetic field saturates both the bottom and the top NiFe layers, while below T_B the BFM bottom layer exhibits a more hard character and needs a few decades Oe to be saturated. As we progressively apply higher magnetic fields the zero-field cooled and field cooled curves merge; eventually at 1 kOe only a minor irreversibility exists which is difficult to be discerned (see the emu range in panel (b)). The fact that the magnetic behavior of the TL changes drastically below T_B may also be revealed by isothermal loop measurements as the ones presented in panel (c). For the sake of clarity the presented data refer only to the decreasing branch of the complete $m(H)$ loops. We clearly see that below $T_B = 90$ K in addition to the reversal of the soft NiFe top layer, which occurs around zero field, a second loop is superimposed with a coercivity that gradually increases as we lower the temperature. This particular second loop is related to the BFM NiFe bottom layer.

We stress that although all data presented in Figs. 1(a)-1(c) show clear indications for the existence of the exchange bias mechanism they refer to the case when the specimens were virgin. However, the fingerprint of unidirectional magnetic anisotropy is a shift observed in

the magnetization loop when the sample is exchange biased i.e. when it is cooled from above the Neel or blocking temperature under the presence of a sufficiently high magnetic field.^{53,54} Such data are presented in Figs. 2(a) and 2(b) for a complete TL (open circles) and a SL (solid circles) at $T = 8 \text{ K} > T_c^{SC}$ when the samples were virgin and BS, respectively. We see that in both cases the magnetization loop of the TL is the superposition of the loop of the BFM bottom SL (shown) and of the PFM top one (not shown). When the samples were biased by cooling them from above $T_B = 90$ K under the presence of $H_{ex} = 1000$ Oe the obtained loops are shifted toward negative fields by 50 Oe. We have to note that the shape of the loop of the BFM SL points rather to a system comprised of hard and soft NiFe phases than an one that constitutes of FM and AFM areas. However, as has been revealed in recent years the underlying physics of exchange coupled hard/soft and FM/AFM systems are essentially the same.^{56,57,58,59,60} For instance, Dieny and colleagues have shown very recently⁵⁷ that in a soft NiFe layer which is exchange coupled with a hard and strongly anisotropic Co/Pt multilayer all the characteristics of exchange bias are met, including shifted magnetization loops, training effects, decreasing bias field with increasing temperature etc. Also, Chien et al.⁶⁰ have revealed that in the archetypal NiFe/FeMn FM/AFM exchange bias system the spins structure in the main body of the AFM layer is not static but due to the coupling with the FM one the spins of the FeMn layer form an exchange spring that may wind and unwind as happens in typical soft/hard BLs. Finally, lately Ali et al. in Ref.61 revealed that the effect of exchange bias has even wider generality since they reported on the observation of this effect in FM/spin glass BLs.

Although we have revealed the fingerprint of exchange bias in our samples, in Figs. 3(a) and 3(b) we present additional magnetization data necessary for a reliable magnetic characterization. Panel (a) shows two successive loops obtained at $T = 8 \text{ K} > T_c^{SC}$, while panel (b) presents minor successive loops at the same temperature. The data presented in panel (a) reveal the so-called training effect (see section 6.6 in Ref.53). The drastic reduction of the loop's width observed in our data indicates that consecutive loops lead to a softening of the underlying physical origin of exchange bias. This result resembles strongly the one obtained by Gruyters and Riegel⁵⁵ in a CoO/Co BL that is considered as a very typical exchange bias system.⁵³ This strong similarity reveals that indeed the hard/soft and FM/AFM systems have similar underlying physical principles;⁵⁹ all the effects observed in both systems are motivated by the exchange coupling occurring at the interfaces of the two different constituents. This is further demonstrated by the data presented in panel (b). While the first part of the loop where the soft NiFe phase reverses its magnetization is reversible, the second part clearly exhibits its irreversible nature associated to the reversal of the hard phase magnetization.

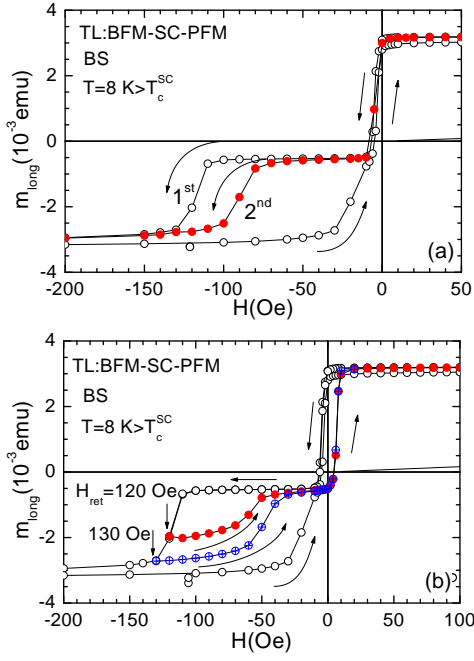


FIG. 3: (Colour online) (a) Complete and (b) minor successive magnetization loops of the longitudinal component obtained at $T = 8 \text{ K} > T_c^{SC}$ for a TL:BFM-SC-PFM.

B. Comparison between transport and magnetization data

Figures 4(a)-4(c) present detailed transport data for a TL:BFM-SC-PFM that were obtained very close to the zero-field critical temperature $T_c^{SC} = 7.81 \text{ K}$ of its SC interlayer. Panel (a) shows the zero-field resistive transition of the TL. The isothermal magnetoresistance $V(H)$ curves presented in panels (b) and (c) were obtained at temperatures allocated across this specific zero-field resistive $V(T)$ curve. Panel (b) presents the obtained curve at $T = 8 \text{ K} > T_c^{SC} = 7.81 \text{ K}$. We see that there is one distinct peak that is positioned at zero field and another minor peak which occurs around -120 Oe . According to the definition $(R_{max} - R_{min})/R_{nor} \times 100\%$ that is commonly used to categorize magnetoresistance effects^{12,13,14,45} the effect observed in the normal state of our TL is very weak: 0.7%. In contrast, when the Nb interlayer becomes SC the effect is strongly enhanced as it is shown in panel (c). While as the applied field is lowered the resistance of the TL is also reduced, for magnetic fields in the range $-200 \text{ Oe} < H < 200 \text{ Oe}$ the measured resistance presents pronounced peaks. These magnetoresistance peaks become maximum at the middle of the zero-field resistive transition (see panel (a)) and gradually diminish as both the normal and the fully superconducting states are recovered. This result was reported very recently in Ref.46 for the same BFM-SC-PFM TLs and reminisces the one reported in Ref.45 for more simple PFM-SC-PFM TLs and the one reported in Refs.12 and 14

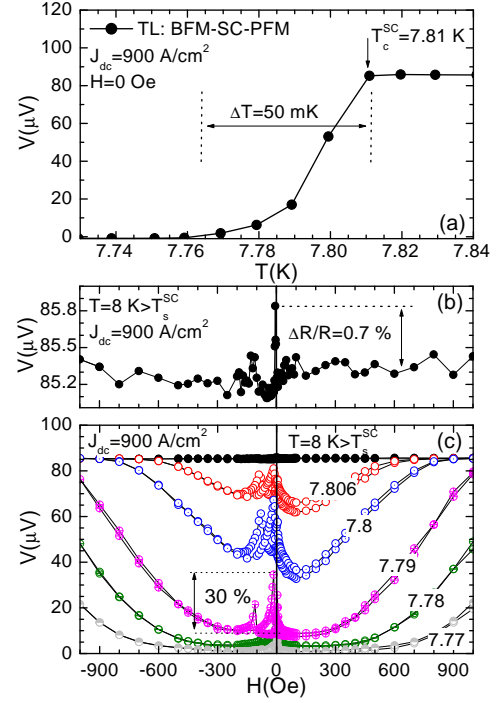


FIG. 4: (Colour online) (a) Zero-field resistive transition of a TL:BFM-SC-PFM with $T_c^{SC} = 7.81 \text{ K}$. (b) Isothermal $V(H)$ curve obtained at $T = 8 \text{ K} > T_c^{SC} = 7.81 \text{ K}$. (c) Isothermal $V(H)$ curves obtained at temperatures allocated across the zero-field isofield resistive $V(T)$ curve presented in panel (a). All the data were obtained when the TL was BS.

for $\text{La}_{0.7}\text{Ca}_{0.3}\text{MnO}_3\text{-YBa}_2\text{Cu}_3\text{O}_{7-\delta}\text{-La}_{0.7}\text{Ca}_{0.3}\text{MnO}_3$ ones. The observed effect is strong. The percentage resistance change $(R(0) - R(H))/R(H) \times 100\%$ meets the quantitative criteria for considered as a giant magnetoresistance (GMR) effect^{2,3,12,14} since according to the modest definition $(R_{max} - R_{min})/R_{nor} \times 100\%$ (that takes into account the reference resistance value obtained in the normal state) it amounts to 50%. We note that this definition should be considered as the most appropriate for the description of the underlying physics since the alternative one $(R_{max} - R_{min})/R_{min} \times 100\%$ (that takes into account the minimum value obtained in the superconducting state) suffers from possible singularities originating from the zeroing of the measured resistance that naturally occurs in every SC.

We note that the $V(H)$ curves presented in Figs.4(b) and 4(c) refer to the case when the TL was BS only *once*, prior to the first measurement. As we show below owing to the training effect⁵³ this measuring procedure leads to significant differences when compared to the one when the specimen gets always BS prior to each new measurement. In addition, these curves differ strongly from the ones obtained for virgin TL. This fact is clearly shown by the comparative data that are presented in Figs.5(a)-5(c) around the zero-field resistive transition of a second BFM-SC-PFM TL that exhibits a slightly higher critical temperature, $T_c^{SC} = 7.89 \text{ K}$. For the sake of clarity

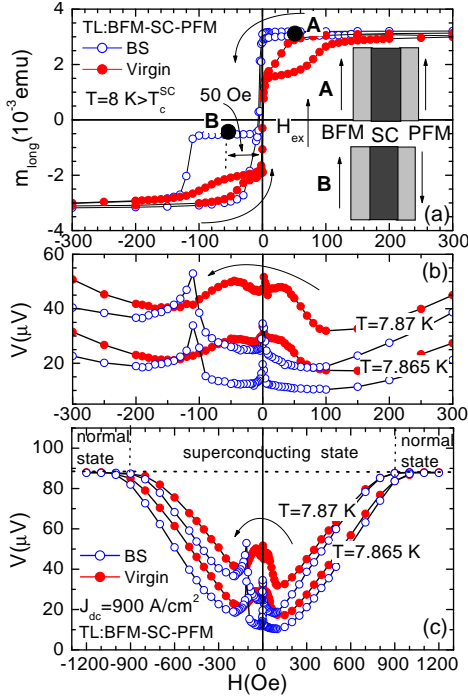


FIG. 5: (Colour online) (a) Detailed magnetization loops of the longitudinal component for virgin (solid circles) and BS (open circles) TL obtained at $T = 8\text{ K} > T_c^{\text{SC}} = 7.89\text{ K}$. Representative magnetoresistance $V(H)$ curves obtained just below the critical temperature $T_c^{\text{SC}} = 7.89\text{ K}$ when the TL was virgin (solid circles) and BS (open circles) in the low-field (b) and in an extended field (c) regime. The insets show schematically the relative in-plane magnetization configuration of the outer FM layers at points A and B of the BS loop.

panel (a) reproduces the detailed magnetization loops for virgin (solid circles) and BS (open circles) TL, while its insets show schematically the relative in-plane magnetization configuration of the outer FM layers at points A and B of the BS loop where $H_{\text{ex}} = 50\text{ Oe}$ and -50 Oe , respectively. Panels (b) and (c) show representative magnetoresistance isothermal data that were obtained at $T = 7.865\text{ K}$ and $T = 7.87\text{ K}$ in the low-field and in an extended field regime, respectively. Both virgin (solid circles) and BS (open circles) curves are shown for each temperature. Firstly, the virgin curve mainly presents a peak around zero field that is significantly broader than the one observed in PFM-SC-PFM TLs as it was reported in Refs.45. An additional second minor peak is also present at exactly zero field. As we see from the virgin magnetization curve $m_{\text{long}}(H)$ presented in panel (a) the two outer NiFe layers reverse their magnetizations in the respective field interval. This result was originally presented in Refs.45,46 and is identical in magnitude to the one presented by Peña et al.¹² and Visani et al.¹⁴ for $\text{La}_{0.7}\text{Ca}_{0.3}\text{MnO}_3\text{-YBa}_2\text{Cu}_3\text{O}_{7-\text{La}_{0.7}\text{Ca}_{0.3}\text{MnO}_3}$ TLs. *More importantly, here we clearly demonstrate that this broad peak centered around zero field may be almost entirely suppressed by the application of exchange bias.* Sec-

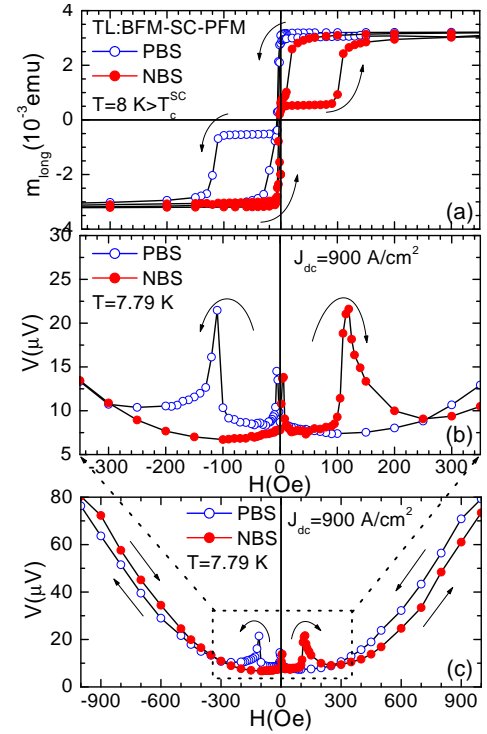


FIG. 6: (Colour online) (a) Magnetization loops of the longitudinal component obtained at $T = 8\text{ K} > T_c^{\text{SC}}$ when the hybrid was positively BS (PBS) and when negatively BS (NBS). (b) and (c) show the respective magnetoresistance $V(H)$ curves obtained at $T = 7.79\text{ K} \approx T_c^{\text{SC}}$ in a focused and in an extended field regime, respectively. In all cases the open circles refer to PBS, while solid circles to NBS condition.

ond, we see that while in the normal state the virgin and BS curves clearly coincide, as we enter in the superconducting state these curves diverge, with the BS curve placed significantly below the virgin one except for a small field regime around the coercive field of the BS bottom NiFe layer (see panel (a)). In addition, the BS magnetoresistance curve exhibits another peak placed at zero field where the plain top NiFe layer reverses abruptly its magnetization. Thus, we see that in both cases, virgin and BS, the obtained magnetoresistance curves present two distinct peaks placed at the field intervals where the two NiFe layers reverse their magnetizations i.e. at the coercive fields. Consequently, according to our results *the extreme dissipation peaks observed in FM-SC-FM TLs are mainly related to the reversal of the outer FM layers' magnetizations rather than their relative in-plane magnetic configuration as it was supposed in Refs.8,9,10,11,12,13,14.* Finally, the maximum value obtained in the BS magnetoresistance curves is equal to the one obtained by the virgin ones. For instance in Fig.5(b) we see that for $T = 7.87\text{ K}$ the maximum value of the BS curve that is achieved at $H_{\text{ex}} = -110\text{ Oe}$ equals the one obtained by the respective virgin curve at $H_{\text{ex}} \approx 0\text{ Oe}$.

In order to further clarify our results and to leave

no doubt that the effects observed in the superconducting state are motivated by the exchange bias we performed additional test experiments. In Figs.6(a)-6(c) we present data when the TL was positively BS (PBS) and when negatively BS (NBS) under the application of $H_{ex} = +1000$ Oe and $H_{ex} = -1000$ Oe, respectively. Since the exchange bias imposes unidirectional magnetic anisotropy the obtained curves should be exact mirror images. This is what we have observed. Panel (a) shows the magnetization loop $m_{long}(H)$ curves of the longitudinal magnetic component, while panels (b) and (c) show the isothermal magnetoresistance $V(H)$ curves that were obtained at $T = 7.79$ K $\approx T_c^{SC}$ in a narrow and in an extended field regime, respectively. We clearly see that both the magnetization $m(H)$ and magnetoresistance $V(H)$ curves that were obtained when the hybrid is NBS are the exact mirror images of the ones obtained when the TL was PBS. These results unexceptionably demonstrate that the unidirectional magnetic anisotropy introduced by the exchange bias dominates the behavior of the whole hybrid even in the superconducting regime below T_c^{SC} .

C. Magnetization data on the transverse component

For the case of PFM-SC-PFM TLs in Ref.45 we have showed that at the same field intervals where the magnetoresistance peaks are observed the magnetizations of the outer FM layers exhibit a significant out-of-plane rotation. As a consequence the SC interlayer below its T_c^{SC} attains a $m(H)$ model loop only in its *transverse* magnetic component, while its *longitudinal* one is almost completely suppressed. This proved that for PFM-SC-PFM TLs the SC interlayer behaves diamagnetically not in respect to the externally applied magnetic field but in respect to the transverse magnetization field originating from the magnetic coupling of the outer FM layers.⁴⁵ Examining this possibility for the case of BFM-SC-PFM TLs could reveal important information regarding the influence of exchange bias. In Fig.7 we present the respective data regarding the transverse magnetic component of a BFM-SC-PFM TL when it was virgin (solid circles) and when BS (open circles). The respective inset shows schematically the experimental configuration between the external field and the TL's magnetic components. Also, shown is the TL's magnetic configuration around zero field for the magnetization loop that is obtained when the TL is virgin. We recall that in this field interval the broad magnetoresistance peaks are observed for the virgin TL (see Figs.5(b)-5(c)). *Interestingly, the respective transverse magnetization data clearly show that in this field interval the out-of-plane magnetic configuration of the outer FM layers is antiparallel.* By comparing to the respective longitudinal magnetic data shown in Fig.5(a) we clearly see that in both virgin and BS cases the reversal of the outer FM layers' magnetiza-

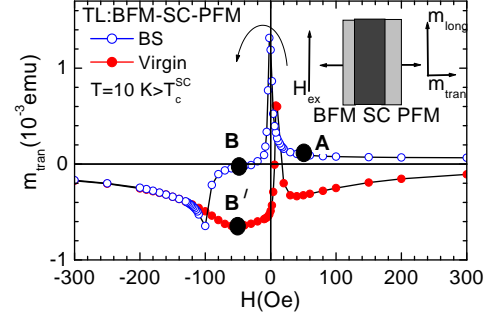


FIG. 7: (Colour online) Detailed magnetization data of the transverse component for virgin (solid circles) and BS (open circles) TL obtained at $T = 10$ K $> T_c^{SC}$. The inset shows schematically the experimental configuration between the external field and the TL's magnetic components. Also, shown is the virgin TL's specific out-of-plane magnetic configuration obtained around zero field where the broad magnetoresistance peaks are observed (see Figs.5(b)-5(c)).

tion is accompanied by a significant out-of-plane rotation occurring across the coercive field. Most importantly, we see that the exchange bias restricts the out-of-plane rotation to a narrow field range around $H_{ex} = -100$ Oe, in contrast to the virgin case where its out-of-plane rotation extends in the whole range of negative fields -200 Oe $\leq H_{ex} \leq 0$ Oe. The respective data of the top PFM layer's magnetization don't show significant differences.

Based on the results shown in Fig.7 we may assume that the dissipation peaks presented in Figs.5(b)-5(c) could be related to the out-of-plane rotation. However, the measurements presented in Fig.7 refer to the *normal* state of the SC interlayer since they were obtained at $T = 10$ K $> T_c^{SC}$. To further examine the effect we performed detailed measurements of the TL's transverse magnetic component in the *superconducting* regime. Complete data are presented in Figs.8(a)-8(b) for temperatures close [upper panel] and well below [lower panel] T_c^{SC} . We clearly see that the TL's transverse magnetic component exhibits the model loop expected for a SC when bulk pinning dominates. Also, we see that in the low-field regime a suppression of the magnetization is observed owing to the out-of-plane rotation of the FM layers' magnetizations.

In contrast, the measured loop of the longitudinal magnetic component in the superconducting state is almost identical to the one observed in the normal regime. The respective data for the longitudinal component obtained at temperatures close and well below T_c^{SC} are shown in Fig.9. We see that the magnetization loop of the complete TL qualitatively reminisces not the one of a SC but that of a FM. It is only well below T_c^{SC} where significant hysteresis shows up in the high field regime. However, close to zero field the typical FM behavior is recovered in all cases. The results presented in Figs.8(a)-8(b) and 9 clearly demonstrate that *the SC behaves diamagnetically not in respect to the externally applied magnetic field but*

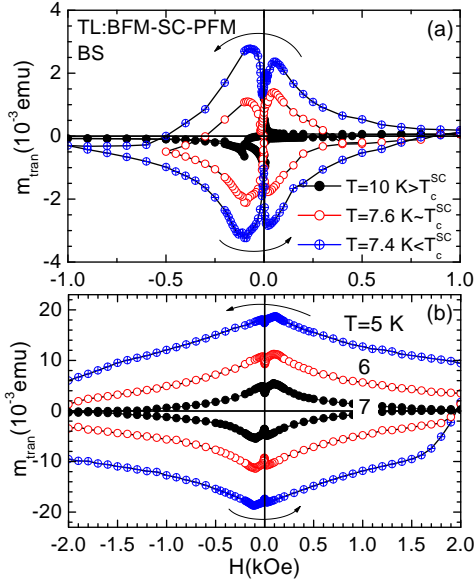


FIG. 8: (Colour online) Detailed magnetization loops of the BS TL's transverse component obtained (a) close to T_c^{SC} and (b) well inside the superconducting state.

in respect to a new transverse magnetic field that obviously emerges due to the magnetic coupling of the outer FM layers (see the discussion below).

Figures 10(a)-10(b) present comparatively low-field transverse magnetization and transport data for a BFM-SC-PFM TL when it is BS for both increasing (solid circles) and decreasing (open circles) the external magnetic field. We clearly see that the morphology of the presented curves is identical: the dissipation peaks occur at exactly the same field values where the transverse component gets maximum. This shows unambiguously that *the dissipation peaks are related to the out-of-plane rotation of the outer FM layers' magnetization*. Consequently, as in the PFM-SC-PFM TLs studied in Ref.45 even for the BFM-SC-PFM TLs studied in this work the pronounced dissipation peaks may be ascribed to the strict influence of the transverse magnetization field that emerge due to the magnetic interconnection of the outer FM layers.

Ultimately, the magnetostatic coupling discussed here could motivate the magnetoresistance peaks that we observe as following: the stray fields that interconnect the outer NiFe layers penetrate completely the Nb interlayer (see Fig.13, below). Depending on the specific characteristics of the employed FM layers (exchange field, size of magnetic domains, width and kind -Neel or Bloch- of domain walls, etc) and of the SC interlayer (lower and upper critical field values, bulk pinning force, etc) the FMs' stray fields will primarily exceed the SC's lower critical field and secondarily, in case that they are intense, even the SC's upper critical field could *locally* be exceeded, at least extremely close to its T_c^{SC} where it attains low values. In case where only the SC's lower critical field is exceeded by the FMs' stray fields dissipation should

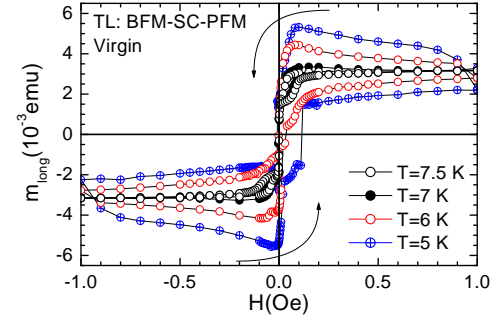


FIG. 9: (Colour online) Detailed magnetization loops of the BS TL's longitudinal component obtained close to T_c^{SC} and well inside the superconducting state.

set in due to flow of vortices that are spontaneously created. As we lower the temperature the magnetoresistance peaks become progressively smaller and eventually disappear since either strong bulk pinning emerges so that vortices are no longer free to move, or the SC's increasing lower critical field exceeds the FMs' stray fields so that a dissipationless Meissner state is ultimately recovered. This explanation resembles the one that was presented by Ryazanov et al. in Ref.42 for Nb-Cu_{0.43}Ni_{0.57} BLs, and by Bell et al. in Ref.43 for all-amorphous GdNi-MoGe-GdNi TLs. Thus, our results extend the ones of Ref.43 to non-amorphous NiFe-Nb-NiFe TLs. In case where also the SC's upper critical field is exceeded the *localized* normal areas that emerge should contribute extra dissipation. Eventually, in this scenario the disappearance of the magnetoresistance peaks is owing to the fact that as we progressively lower the temperature the SC's upper critical field exceeds the stray fields that interconnect the outer FMs so that bulk superconductivity is completely restored throughout the whole SC interlayer. Of course, since the SC's lower critical field is always smaller than its upper critical one we expect that the mechanism described in the former [latter] case should have a major [minor] contribution to the observed magnetoresistance effect.

D. FM-SC-FM TLs: comparison with current experiments

As already discussed in the "Introduction" specific discrepancies have been reported in the recent literature^{8,9,10,11,12,13,14,46} regarding the operation of relevant FM-SC-FM TLs. Such TLs have been considered as superconducting "spin valves" both theoretically (see Refs.16,17) and experimentally (see Refs.8,9,10,11,12,13,14). We stress that we use the quotation marks since according to the results of this work the physical mechanism motivating the pronounced magnetoresistance peaks is not actually related to a spin-dependent pair-breaking effect as it was theoretically pro-

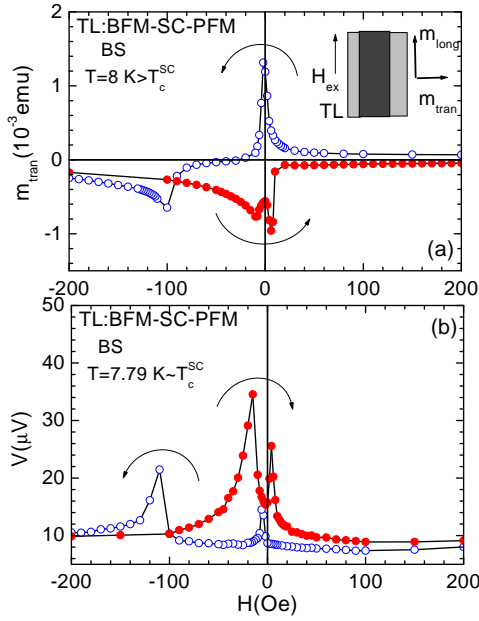


FIG. 10: (Colour online) Comparative presentation of the low field transverse magnetic component (a) and magnetoresistance curve (b) for a BS TL obtained at $T = 8 \text{ K} > T_c^{SC}$ and at $T = 7.79 \approx T_c^{SC}$, respectively. Both increasing (solid circles) and decreasing (open circles) branches are shown. The inset shows schematically the experimental configuration between the external field and the TL's magnetic components.

posed in Refs.16,17. According to our results the magnetoresistance peaks originate mainly from the suppression of the SC interlayer's properties owing to the stray fields that interconnect the outer FM layers, or in other words owing to their out-of-plane magnetic configuration. Thus, the experiments of Refs.8,9,10,11,12,13,14,46 should be reconsidered as being realizations of the theoretical proposals presented in Refs.16,17. In the discussion that follows we temporarily neglect the new experimental results presented in this work regarding the influence of the FMs' out-of-plane magnetization field on the properties of the SC interlayer in order to make a brief overview of the recent experimental works (see Refs.8,9,10,11,12,13,14,46) and to ultimately suggest an explanation that is consistent with both the already available data (see Refs.8,9,10,11,12,13,14,46) and the new results that we present. For the moment we will assume that only the in-plane relative magnetization configuration of the outer FM layers controls the properties of the SC interlayer and we will adopt the point of view proposed in Refs.8,9,10,11,12,13,14,46.

1. Considering only the in-plane relative magnetization configuration

While some works argued that the antiparallel [parallel] in-plane magnetization configuration of the outer

FM layers promotes [suppresses] superconductivity (see Refs.8,9,10,11), others have provided evidence for exactly the opposite behavior where the antiparallel [parallel] in-plane magnetization configuration of the outer FM layers suppresses [promotes] superconductivity (see Refs.12,13,14,46). In order to investigate this discrepancy we performed additional experiments. Representative results are shown in Figs.11(a)-11(c). First, these data reveal that *the exchange bias clearly promotes the resistive critical temperature of the TL* as for instance may be seen in panel (a) where both $V(T)$ curves were obtained for the same external field $H_{ex} = -50 \text{ Oe}$. The data shown in panels (b) and (c) were obtained for opposite external fields $H_{ex} = -50 \text{ Oe}$ and $H_{ex} = 50 \text{ Oe}$ and refer to BS and virgin TL, respectively. The two cases of the relative in-plane magnetization configurations of the outer FM layers are realized: in both panels (b) and (c) the antiparallel [solid lines] occurs for $H_{ex} = -50 \text{ Oe}$ and the parallel [dotted lines] is obtained for $H_{ex} = 50 \text{ Oe}$. Of course, the antiparallel configuration is more robust for the BS case as it is presented in points A and B that refer to the BS loop shown in Fig.5(a). We see that whether the bottom NiFe layer is BS [panel (b)] or virgin [panel (c)] the antiparallel [$H_{ex} = -50 \text{ Oe}$] in-plane magnetization configuration of the outer FM layers places the resistive transition at lower temperatures compared to the case when the NiFe layers are parallel [$H_{ex} = 50 \text{ Oe}$]. The same results were obtained for all field values in the interval $-100 \text{ Oe} < H_{ex} < 100 \text{ Oe}$, where the antiparallel and parallel in-plane magnetization configuration is realizable. Finally, we have to stress that the data presented in Figs.11(a)-11(c) clearly prove that *the observed effects are an exclusive property of the superconducting state since in the normal state, i.e. for $T > T_c^{SC}$, the resistance curves clearly coincide*.

Since in the measurements presented in Figs.11(a)-11(c) the observed temperature shifts are very small but, at least, comparable to the ones presented in Refs.8,9,10,11,12,13 we performed some test measurements in order to ensure that these shifts are motivated by the physics of the studied systems and are not artifacts. The results of Figs.12(a)-12(b) serve this aim. Panel (a) clearly shows that when the TL is virgin, at the symmetric points $H_{ex} = -300 \text{ Oe}$ (dashed line) and 300 Oe (solid line) of the magnetization loop (see the virgin loop in Fig.5(a)) the obtained $V(T)$ curves clearly coincide as they should. In addition, in the same panel presented is the respective curve obtained at $H_{ex} = 300 \text{ Oe}$ (dotted line) when the TL was positively BS (PBS), i.e. under the application of a positive magnetic field. Clearly the PBS resistive curve is placed at higher temperatures compared to the virgin ones. Panel (b) shows test data obtained for $H_{ex} = 50 \text{ Oe}$ and -50 Oe when the TL was PBS (positively BS) and NBS (negatively BS). The respective $m(H)$ loops are presented in Fig.6(a). Since the observed divergence of the two curves is below 1 mK we may assume that the obtained $V(T)$ curves coincide as they should.

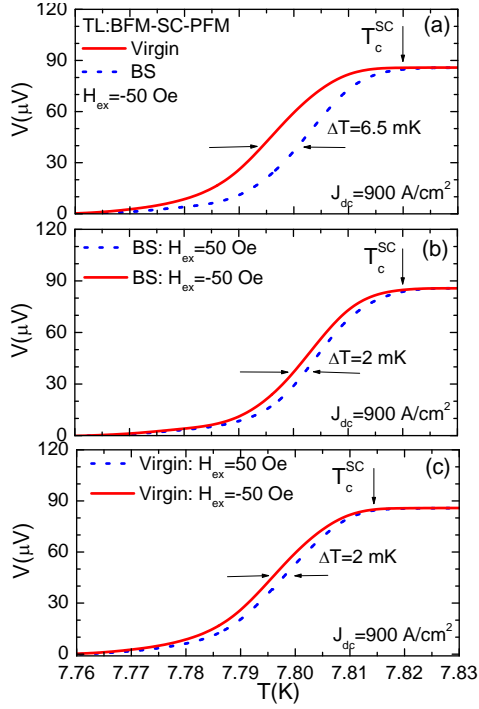


FIG. 11: (Colour online) Representative voltage curves as a function of temperature (a) at $H_{ex} = -50$ Oe when the TL is virgin (solid line) and BS (dotted line), (b) at $H_{ex} = -50$ Oe (solid line) and 50 Oe (dotted line) when it is BS, and (c) at $H_{ex} = -50$ Oe (solid line) and 50 Oe (dotted line) when it is virgin.

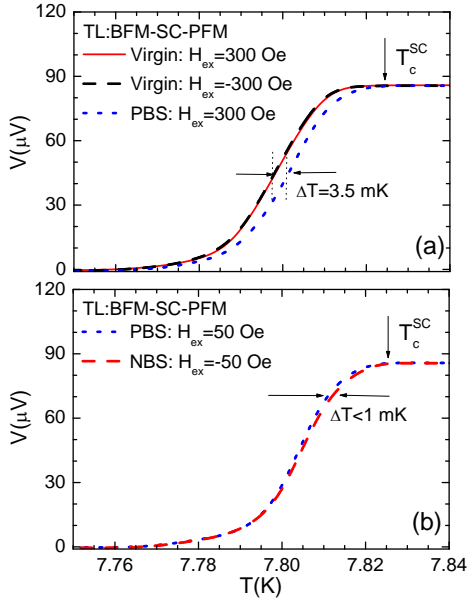


FIG. 12: (Colour online) (a) Magnetoresistance curves obtained at the symmetric points $H_{ex} = -300$ Oe (dashed line) and 300 Oe (solid line) of the virgin TL's magnetization loop (see the virgin loop in Fig.5(a)) and the respective curve obtained at $H_{ex} = 300$ Oe (dotted line) when the TL was positively BS. (b) Test magnetoresistance data obtained for $H_{ex} = 50$ Oe and -50 Oe when the TL was positively (dotted line) and negatively (dashed line) BS (see the respective loops in Fig.6(a)).

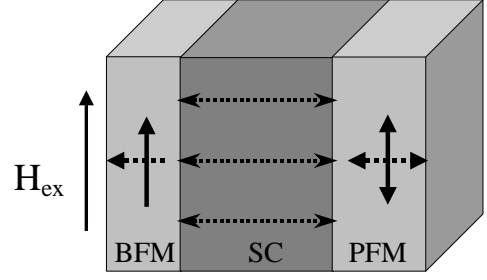


FIG. 13: (Colour online) Schematic representation of how the outer FM layers may influence the SC interlayer. In most experiments the BFM layer that is employed has a robust magnetization due to pinning by exchange bias. In contrast, the magnetization of the PFM layer is free to rotate. In our samples both the in-plane (solid arrows) and out-of-plane (dotted arrows) relative magnetization configurations of the outer FM layers are present and influence the transport properties of the SC interlayer.

According to the point of view adopted in Refs.8,9, 10,11,12,13,14,46 where only the in-plane relative magnetization configuration of the FMs was considered our results support the experimental outcome of Refs.12,13, 14,46 where it was concluded that the antiparallel [parallel] in-plane magnetization configuration of the outer FM layers suppresses [promotes] superconductivity. However, in this work we clearly show that the underlying mechanism motivating the magnetoresistance peaks is surely related to the *out-of-plane* rotation of the magnetizations of the outer FM layers and not only to their *in-plane* relative configuration. The combination of both the in-plane and out-of-plane relative magnetization configuration is schematically presented in Fig.13. Thus, it is now easy to explain all the available experimental data presented in Refs.8,9,10,11,12,13,14 and in this work.

2. Considering both the in-plane and out-of-plane relative magnetization configuration

First, let us consider the results presented in Fig.11(a) in comparison to the ones of Fig.7. In Fig.11(a) both curves were obtained for $H_{ex} = -50$ Oe but the BS curve is placed significantly above the virgin one; $\Delta T = 6.5$ mK. Figure 7 reveals that at $H_{ex} = -50$ Oe when the TL is virgin a significant part of its magnetization rotates out-of-plane, while when it is BS the in-plane magnetic order is preserved so that its transverse component is zero (see points B' and B in Fig.7, respectively). Thus, the transverse magnetic component of the outer FMs could strongly influence the SC interlayer only for the virgin case, while for the BS one its influence (if any) should be minimum.

On the other hand the data presented in Fig.11(b) refer to the case when although the TL is always BS the external field's polarity is opposite ($H_{ex} = 50$ Oe vs -50 Oe).

Oe). According to the results of Fig.7 for these two cases the difference of the out-of-plane magnetic component is only minor (see points A and B in Fig.7). This is the reason why the initial temperature shift of $\Delta T = 6.5$ mK between the curves presented in Fig.11(a) decreases down to $\Delta T = 2$ mK for those presented in Fig.11(b). By making the assumption that in both cases presented in Fig.11(b) the transverse component is almost identical (see points A and B in Fig.7) we may attribute the observed shift of $\Delta T = 2$ mK exclusively to the in-plane relative magnetization configuration of the outer FM layers. Under this assumption our results are compatible to the ones presented in Refs.12,13,14 and 46 where it was concluded that the antiparallel [parallel] in-plane magnetization configuration of the outer FM layers suppresses [promotes] superconductivity. However, as we demonstrate here small temperature shifts ($\Delta T = 2$ mK) of the resistive curves which are motivated mainly by the relative in-plane magnetization configuration of the outer FM layers are enhanced ($\Delta T = 6.5$ mK) under the influence of the out-of-plane rotation of their magnetizations.

3. Prerequisite for intense stray-fields magnetoresistance in FM-SC-FM TLs

The results that were presented until now and the discussion made just above prove that since three parameters do get involved in such hybrid TLs: (i) the out-of-plane magnetizations' rotation and the unavoidable stray-fields coupling of the outer FM layers, (ii) the in-plane relative magnetization configuration of the outer FM layers, and (iii) the direct or indirect influence of exchange bias, the small temperature shifts that are observed should not be ascribed exclusively to the one of them, namely the in-plane relative magnetic configuration, as it was suggested in Refs.8,9,10,11,12,13,14 and 46.

Since we reveal the significance of the out-of-plane magnetic component that is related to the stray fields emerging at magnetic domain walls around coercivity, in this subsection let us first make a brief overview of the literature related with this topic. Subsequently, we propose a plausible explanation that in a phenomenological level explains naturally all the recent experimental works.

Parallel field configuration: First we discuss the configuration where the external field is applied *parallel* to a FM-SC hybrid as in the present work. The influence of stray fields that originate from a FM multilayer on an adjacent SC was already highlighted in Refs.20,21,22. Also, the influence of stray fields in FM-SC MLs was reported very recently in Ref.38. However, for more simple structures as the FM-SC-FM TLs studied in the present article the dominant influence of stray-fields coupling of the outer FM layers on the SC interlayer has been proven very recently in Refs.44,45 for the case of FM-SC-FM TLs when the external magnetic field was applied *parallel* to their surface. Detailed discussion on the possi-

ble underlying mechanism that eventually suppresses the transport properties of the "magnetically pierced" SC interlayer was made above (see subsection III.C).

Normal field configuration: On the other hand the case of FM-SC-FM TLs where the magnetic field was applied *normal* to their surface it was studied in Refs.15 and 39 for Co-Pt/Nb/Co-Pt and Co-Pd/Nb/Co-Pd, respectively. Unfortunately, in these works^{15,39} complete transport data that would reveal the behavior of the TL as the magnetic field is scanned from positive to negative saturation of the FM layers were not presented. Thus, the exact transport behavior around the FM's coercive fields is still not clear for the normal-field configuration. More specifically, Singh et al. in Ref.15 contrasted their results with the ones presented by Gillijns et al. in Ref.39, and claimed that stray fields were not involved in their experiments as this was evidenced when an insulating SiO₂ layer was introduced at each FM-SC interface so that the electronic coupling of the two constituents was removed. However, in the specific transport experiments that were presented in Ref.15 each FM layer was in its saturated magnetic state so that possible stray fields were only limited at the specimen's edges. This specific magnetic realization was employed successfully long time ago in Ref.65 as the critical current of a SC strip was controlled by the stray fields that were restricted at the edges of a homogeneously magnetized FM layer that was adjacent to the SC through a thin oxide interlayer.

We have to stress that in our work we refer not to the stray fields that exist *only near the edges* of a homogeneously magnetized FM as it was discussed in Refs.15,65 but to the stray fields that emerge naturally *all over the surface* of the FM owing to the appearance of magnetic domains around its coercivity. This is a very important difference that should not be disregarded. Here, based on this stray-fields concept we propose a plausible explanation that should hold for both the parallel and normal field configurations and could efficiently capture all the available experimental data presented in the recent literature (see Refs.8,9,10,11,12,13,14 and 44,45,46).

Intuitively, in a FM-SC-FM TL the magnetic coupling of the outer FM layers mediated by the stray fields that emerge naturally near coercivity should be maximum when the coercive fields of the FMs are almost equal.⁶⁴ When this condition is fulfilled the two FM layers are susceptible to get magnetically coupled by the stray fields accompanying the magnetic domains that emerge *simultaneously* all over the surface of both FM layers around their common coercive field. This proposition explains naturally the occurrence of pronounced magnetoresistance peaks in Refs.12,14,44,45. In all these works the FM layers participating a TL had almost identical coercive fields as this is evidenced by the only minor two-step behavior observed in the presented $m(H)$ loops. In contrast, when the coercive field of the first FM layer is significantly different than that of the second one the stray-fields magnetic coupling is not intense so that the magnetoresistance effect is getting weak. This is evidenced by

the experimental results presented in Refs.8,9,10,11,13. In Ref.13 the two FM layers exhibit a few tens Oe different coercive fields as this is clear by the distinct two-step behavior in the presented $m(H)$ loops. Furthermore, in Refs.8,9,10,11 the coercive fields of the outer FM layers differ by several hundreds Oe. Summarizing these data, compared to the magnetoresistance effect reported in Refs.12,14,44,45, where the FM layers share almost common coercive fields, the one reported in Ref.13, where distinct coercive fields of the FMs are clearly resolved, is weaker. Eventually, in Refs.8,9,10,11, where the coercive fields are very different, notable magnetoresistance peaks were not reported. Thus, it is natural to assume that when the coercive regimes of the two FM layers exhibit significant overlapping the observed magnetoresistance effect is pronounced, while as the coercivities get progressively different the magnetoresistance peaks eventually disappear. We believe that the only mechanism that could be invoked for the consistent interpretation of all these experimental data that are reported in the recent literature^{8,9,10,11,12,13,14,44,45,46} is the stray-fields coupling of the outer FM layers that "pierces" magnetically the SC interlayer as it was discussed in Ref.45 for plain TLs and in this work for exchange biased ones (see subsection III.C).

Now, the question that waits for an answer is what is the exact role of the exchange bias mechanism in the BFM-SC-PFM TLs that are studied in our work for the parallel field configuration? We believe that the answer relies on the physical origin of exchange bias and could be given by simple phenomenological arguments. Since the exchange bias induces an in-plane unidirectional anisotropy it also controls the magnetic in-plane order of the TL's bottom BFM layer.⁵³ Thus, when the bottom layer is BS it maintains an in-plane magnetization for a wider field range so that it doesn't exhibit significant out-of-plane rotation, an ingredient that is necessary for the occurrence of broad dissipation peaks. In this case the dissipation peaks are restricted in a narrow field regime around the coercive field. In contrast, when the bottom BFM layer is not exchange biased it is free to attain a significant out-of-plane component. Thus, its magnetic interconnection with the other PFM layer may be achieved easily and the broad dissipation peaks evolve. Finally, as it was proposed in Ref.64 and discussed right above the stray-fields coupling of the outer FM layers should be more efficient under a specific prerequisite: when the FMs share almost common coercive fields. Under this sense *the exchange bias may be considered as a parameter that tunes the coercive field of the one FM layer so that the stray-fields coupling may be controlled through the realization of this specific prerequisite.*

We stress that in even more simple FM-IN-FM and FM-NM-FM TLs (IN and NM stand for insulator and non magnetic metal, respectively) both in-plane and out-of-plane magnetic mechanisms are getting involved. For instance, for the parallel field configuration in FM-IN-FM and FM-NM-FM TLs magnetostatic interactions of

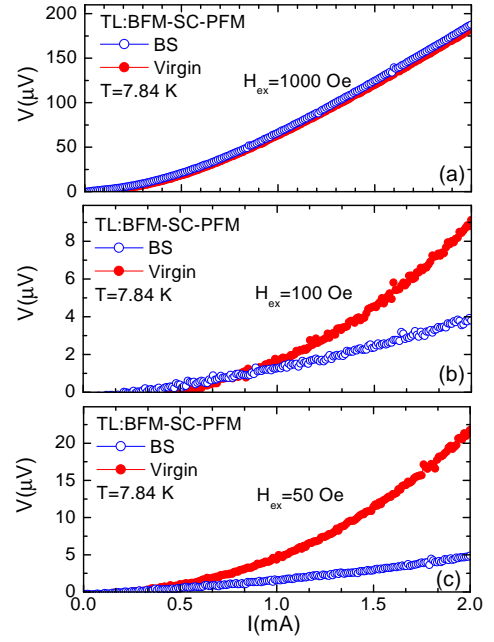


FIG. 14: (Colour online) I-V characteristics obtained at temperature $T = 7.84$ K and for magnetic fields (a) $H_{ex} = 1000$, (b) 100 and (c) 50 Oe. Data that were obtained for both virgin (solid circles) and BS (open circles) bottom NiFe layer are presented.

the outer FM layers through stray fields that occur at domain walls could lead to their significant coupling. Indeed, S. Parkin and colleagues have shown^{4,47} that such stray-fields coupling occurring at domain walls plays a unique role in FM-IN-FM and FM-NM-FM TLs since it vitiates potentially the distinct magnetic character of even quite different outer FM layers. In addition, the action of stray fields could also be promoted by roughness that probably exists at the interfaces (whether it is correlated or not).^{45,48,49}

E. Dynamic behavior through I-V characteristics

In all the data presented so far we have shown that the exchange bias promotes the superconducting properties of the complete hybrid when compared to the case where the bottom NiFe layer is virgin. Important information for the dynamic transport behavior of our hybrids may be gained by measuring I-V characteristics. Representative data are shown in Figs.14(a)-14(c) for the specific temperature $T = 7.84$ K and for magnetic fields $H_{ex} = 1000, 100$ and 50 Oe. We clearly see that close to the normal state i.e. for $H_{ex} = 1000$ Oe there is no actual distinction between the virgin (solid circles) and BS (open circles) I-V curves. But as the applied field is lowered i.e. as we enter deeper in the superconducting state we clearly see that the BS I-V characteristics are placed much lower than the virgin ones. This result re-

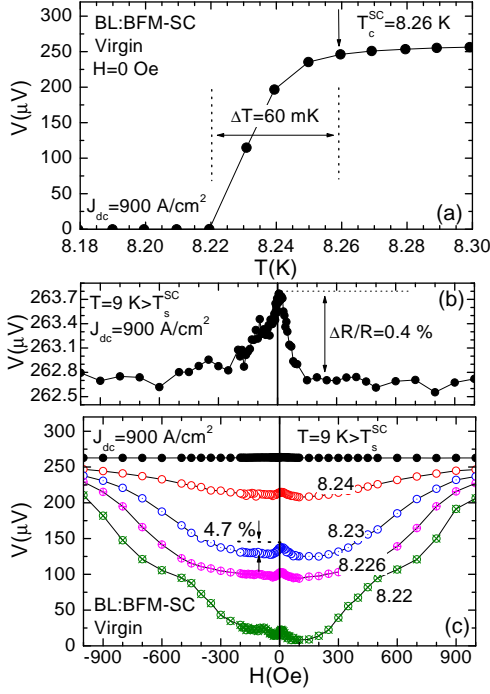


FIG. 15: (Colour online) (a) Zero-field resistive transition of a BL:BFM-SC with $T_c^{SC} = 8.26$ K. (b) Isothermal $V(H)$ curve obtained at $T = 9$ K $> T_c^{SC} = 8.26$ K. (c) Isothermal $V(H)$ curves obtained at temperatures allocated across the zero-field isofield resistive $V(T)$ curve presented in panel (a). All the data were obtained when the BL was virgin.

veals that the current-carrying capability of the complete hybrid is strongly enhanced when the bottom NiFe layer is BS compared to when it is virgin.

IV. EXCHANGE BIASED BLS

A. Comparison between transport and magnetization data

Until now all the data that have been presented referred to BFM-SC-PFM TLs. We have clearly shown that in these structures three parameters mainly control the magnetoresistance peaks that are observed in the low-field regime, close to T_c^{SC} : (i) the out-of-plane rotation of the outer FM layers' magnetizations, subsequently motivating their magnetic interconnection, (ii) the in-plane relative magnetization configuration of the outer FM layers, and (iii) the mechanism of exchange bias that controls the magnetic order of the BFM bottom layer. The investigation of more simple BFM-SC BLs could provide important information on these topics when contrasted to the results obtained in the BFM-SC-PFM TLs since in BLs parameter (ii) is absent and parameter (i) is weakened. In the present work we have made such a detailed investigation. Represen-

tative transport data for a BFM-SC BL that exhibits $T_c^{SC} = 8.26$ K are shown in Figs.15(a)-15(c). Panel (a) shows its zero-field resistive $V(T)$ curve along which the detailed isothermal $V(H)$ curves have been obtained. Panel (b) shows reference data obtained in the normal state i.e. at $T = 9$ K $> T_c^{SC} = 8.26$ K. We see that the obtained curve exhibits a single relatively broad peak placed around zero field. In this field interval the virgin NiFe layer reverses its magnetization (see Fig.16 below). Panel (c) presents the respective $V(H)$ curves obtained at temperatures allocated across the zero-field resistive $V(T)$ curve presented in panel (a). In qualitative agreement with the normal state $V(H)$ curve shown in panel (b) the $V(H)$ ones of panel (c) exhibit one single peak that is placed around zero field. Quantitatively, the situation is different since the magnetoresistance peaks observed in the superconducting (normal) state of the BLs amount to almost 5% (0.4%) according to the definition $(R_{max} - R_{min})/R_{nor} \times 100\%$. We stress that the normal state $V(H)$ curve is presented once again in panel (c): in this range the minor normal state peak ($\Delta R/R_{nor} \times 100\% = 0.4\%$) is not even discerned.

Finally, we note that an oscillating-like behavior observed not only in the virgin (see the curve obtained at $T = 8.22$ K in Fig.15(c)) but also in the BS (see Figs.16(c) and 19(c), below) $V(H)$ curves near the bottom of the zero-field resistive $V(T)$ curve is not understood at the moment. Measurements focused on this effect are on the way and will be discussed in a forthcoming publication.

Until now the $V(H)$ data presented in Fig.15(c) referred to the case where the BL was virgin. A direct comparison between data obtained when the BFM-SC BL is virgin (solid circles) and when BS (open circles) is shown in Figs.16(a)-16(c). Panel (a) shows detailed magnetization loops obtained at $T = 9$ K $> T_c^{SC}$, while panels (b) and (c) show the respective magnetoresistance data in the low-field and in an extended field regime, respectively. Let us first discuss the magnetization data shown in panel (a). A close inspection of the virgin loop reveals that *when the positive part of the decreasing branch is merged with the negative part of the increasing one a complete typical loop of a soft FM is formed* (as presented by the thick solid curve). Thus, we may conclude that when we decrease the applied field from positive saturation it is the soft NiFe areas that firstly reverse their magnetization and subsequently the hard areas also reverse. In the same way when we increase the applied field from negative saturation again the soft (hard) areas reverse first (second). In contrast, when the NiFe layer is BS the two different areas get strongly exchange coupled so that they reverse simultaneously. In the decreasing branch, the point where the abrupt switching of the strongly coupled soft/hard areas occurs in the BS curve coincides with the field value where the gradual reversal of the free/uncoupled *hard* phase is accomplished in the virgin curve. In the increasing branch, the abrupt switching of the BS curve coincides with the point of the virgin curve where the magnetization reversal of the

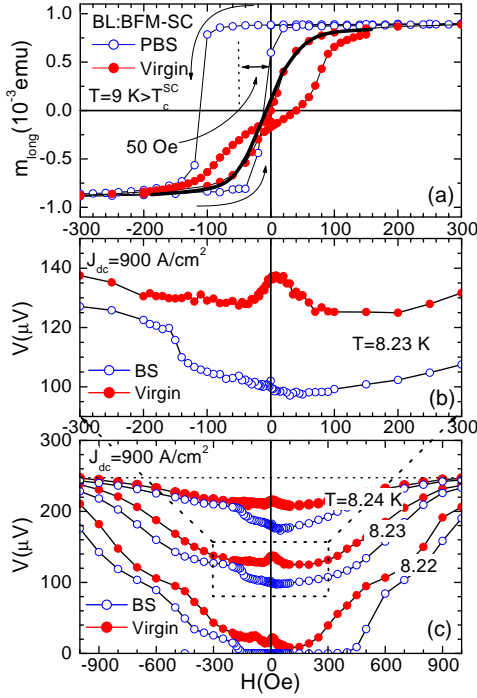


FIG. 16: (Colour online) (a) Detailed magnetization loops for virgin (solid circles) and exchange biased (open circles) BL. (b) Low-field part of a representative magnetoresistance $V(H)$ curve obtained at around the middle of the zero-field resistive transition (see Fig.15(a)) when the BL was virgin (solid circles) and when BS (open circles). (c) Detailed magnetoresistance $V(H)$ curves obtained just below the critical temperature $T_c^{\text{SC}} = 8.26 \text{ K}$ when the BL was virgin (solid circles) and when BS (open circles) in an extended field regime.

free/uncoupled *soft* phase is completed. Thus, when the soft and hard areas are exchange coupled it is the hard phase that determines the point where the switching will take place for the preferential coupling direction imposed initially by the external applied field, while the soft phase determines the switching field in the opposite direction.

Now we may discuss the $V(H)$ curves presented in panels (b) and (c). The virgin $V(H)$ curves present a minor peak as already discussed above. Interestingly, this peak that originally is centered around zero field may be shifted to negative field values under the application of exchange bias. More importantly, we see that while in the normal state the virgin and BS curves coincide, as we enter in the superconducting state these curves diverge, with the BS curve placed significantly below the virgin one in the whole field range; a clear experimental proof that, apart from the TJs, also in the BLs the exchange bias promotes the superconducting properties of the whole hybrid. A clear difference between the data obtained for the BLs (Figs.16(a)-16(c)) and the TJs (Figs.5(a)-5(c)) is the following: while in the BLs the BS curves are placed below the virgin ones in the whole field range, in the TJs there is a small field interval where the BS $V(H)$ curves overshoot the virgin ones. Most im-

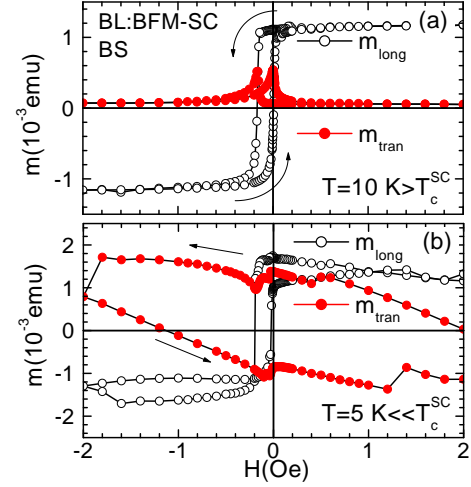


FIG. 17: (Colour online) Representative magnetization loops of the BS BL's longitudinal (open circles) and transverse (solid circles) components obtained (a) above T_c^{SC} and (b) well inside the superconducting state.

portantly, the magnetoresistance peaks observed in the TJs are pronounced [$(R_{\text{max}} - R_{\text{min}})/R_{\text{nor}} \times 100\% = 50\%$] when compared to the ones occurring in the BLs [$(R_{\text{max}} - R_{\text{min}})/R_{\text{nor}} \times 100\% = 5\%$]. We ascribe this significant difference to the fact that the underlying mechanism motivating this effect in the TJs is the magnetic coupling of the outer layers through stray fields as the out-of-plane rotation of their magnetizations takes place near coercivity. On the other hand although in the BLs the out-of-plane rotation of the single BFM layer's magnetization also takes place near coercivity the mechanism of stray fields' interconnection is not possible.

However, the magnetization data presented in Figs.17(a)-17(b) for another BL clearly demonstrate that even in the BLs the out-of-plane rotation of the single BFM layer's magnetization also occurs we believe that this fact deserves a little more attention. This fact is not surprising since the reversal of a FM layer's magnetization usually evolves not only through the formation and movement of magnetic domains but also through the in-plane or, as in our case the out-of-plane rotation of the magnetization. A couple of interesting observations that can be made from the presented data are the following: First, in panel (a) we see that in the normal state the transverse component's maximum (solid circles) occurs at exactly the coercive field of the longitudinal one (open circles). Second, in panel (b) we see that in the superconducting state neither the longitudinal nor the transverse component exhibit the model loop expected for a SC. In contrast, for the TJ the transverse component exhibited the fingerprint of a SC's model $m(H)$ loop (see the detailed loops presented in Figs.8(a)-8(b)). We attribute this difference to the magnetic interconnection of the outer FM layers that in the TJs forces the SC to behave diamagnetically not in respect to the externally

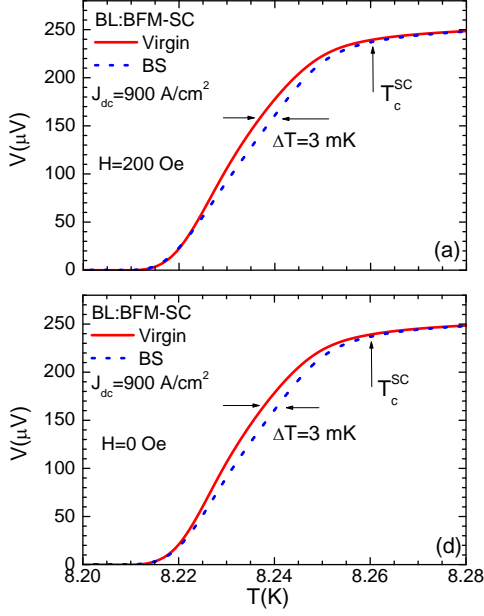


FIG. 18: (Colour online) Representative voltage curves as a function of temperature at (a) $H_{ex} = 200$ Oe and at (b) $H_{ex} = 0$ Oe, when the BL was virgin (solid lines) and when BS (dotted lines).

applied parallel magnetic field but in respect to the transverse magnetization field that emerges. Although in the BLs this exact mechanism is missing the observed magnetoresistance peaks that are shifted from zero field to negative coercivity (see Fig.16(c)) may also be attributed to the out-of-plane rotation of the BL's magnetization that occurs at exactly the same field value.

Except for the isothermal measurements as a function of magnetic field the influence of exchange bias is also identified in the isofield measurements as function of temperature. In Figs.18(a) and 18(b) we show representative data for a BFM-SC BL for the cases when the BL was virgin (solid lines) and when BS (dotted lines). Panel (a) shows the results obtained for external field $H_{ex} = 200$ Oe, while panel (b) for $H_{ex} = 0$ Oe. We see that as we observed in the BFM-SC-PFM TLs also in the BFM-SC BLs the BS state promotes superconductivity when compared to the virgin one. Also, these data clearly prove that the observed effect is an exclusive property of the superconducting state since in the normal state i.e. for $T > T_c^{SC}$ the different resistance curves clearly coincide. Thus, the enhancement of the superconducting properties of the BL can't be attributed to a normal state property of the BFM layer that is preserved in the superconducting state. It is a unique property that is exclusively ascribed to the synergy of superconductivity and exchange bias.

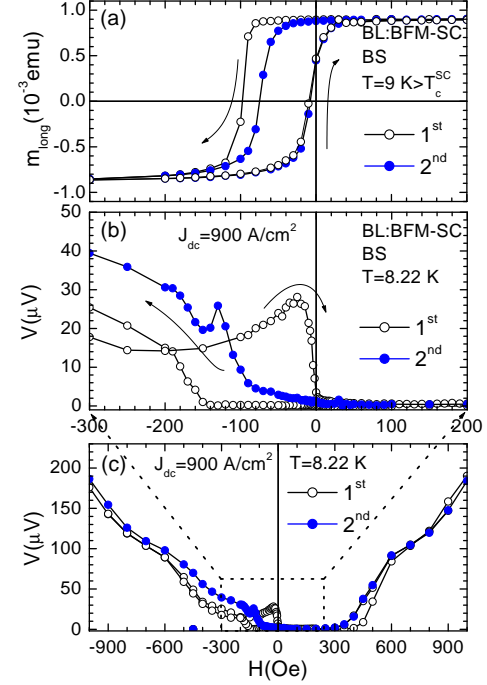


FIG. 19: (Colour online) (a) Two successive magnetization loops obtained at temperature $T = 9$ K $> T_c^{SC}$ in a BFM-SC BL. Successive magnetoresistance $V(H)$ curves obtained at $T = 8.22$ K near the bottom of its zero-field resistive $V(T)$ curve (see Fig. 15(a)) in the low field (b) and in an extended field (c) regime. All the data were obtained during a single run while the BFM-SC hybrid was BS only once, prior to the first loop.

B. Training effect in the superconducting state

As it was discussed in subsection III.A where we presented a complete magnetic characterization of the produced samples one effect that is commonly observed in FM/AFM⁵⁵ and soft/hard⁵⁷ exchange coupled systems is the so-called training effect (see Fig.3(a)).⁵³ According to this effect in an exchange coupled system the shift of the magnetization loop is decreased when successive loops are performed without refreshing the coupling of the FM and AFM constituents by appropriate field cooling from above the Neel or blocking temperature.⁵³ In Fig.3(a) we presented two successive magnetization loops for a TL's longitudinal component that were obtained above the superconducting critical temperature.

In order to investigate if this effect also survives *inside* the superconducting state we performed systematic transport measurements. Figures 19(a)-19(c) show representative data obtained in a BFM-SC BL. Panel (a) shows two successive magnetization loops obtained at temperature $T = 9$ K $> T_c^{SC}$, while panels (b) and (c) show the respective magnetoresistance $V(H)$ curves obtained at $T = 8.22$ K near the bottom of its zero-field resistive $V(T)$ curve (see Fig. 15(a)). Panel (b) focuses in the low-field regime, while panel (c) shows an extended

field range. We note that these data were obtained when the BL was initially BS. In addition, these data have been obtained successively i.e. without refreshing the exchange coupling in the BFM NiFe layer. In panel (a) we see that the width ($W = 95$ Oe), and accordingly the shift, of the loop is decreasing strongly during the second round ($W = 75$ Oe). In addition, in our case we observe that the first decreasing branch is more square-like, while the subsequent one is more rounded. This fact indicates that the underlying mechanisms motivating the reversal of the BFM NiFe layer's magnetization during the first and the subsequent loop is different. Moreover, we see that the increasing branches clearly coincide in all successive rounds, a sign of different magnetization reversal mechanisms between the increasing and decreasing branches.

Panel (b) focuses on the $V(H)$ data in the same field range as in panel (a) in order to make a direct comparison between the longitudinal magnetic component $m_{long}(H)$ and the magnetoresistance $V(H)$ data. We see that during the first turn (open circles) the whole hybrid is superconducting, since it exhibits zero resistance, down to -150 Oe where the first reversal of the NiFe layer's magnetization is completed. At this field the $V(H)$ curve gets non-zero since an abrupt increase is observed for higher negative field values. The return $V(H)$ branch also presents an interesting behavior. While for negative magnetic fields the BFM-SC hybrid superconducts only partially it is just below zero field where it presents a clear peak and abruptly the hybrid becomes completely superconducting since its resistance vanishes at the field where the reversal of the NiFe layer's magnetization is completed. Subsequently, the second decreasing $V(H)$ branch (solid circles) behaves qualitatively similar to the first one (open circles) with the only quantitative difference that it becomes partially superconducting at a lower field value when compared to the first decreasing curve (the abrupt increase occurs at -90 Oe and -150 Oe for the first and second rounds, respectively). This is the fingerprint of the training effect that according to our data survives in the superconducting state.

Panel (c) shows the $V(H)$ curves presented in panel (b) in an extended field range. We see that apart from a small interval of positive magnetic fields the second decreasing $V(H)$ curve (solid circles) is placed above the first one (open circles). This means that in our BFM-SC BLs the exchange bias is an essential ingredient for maintaining the lower resistance that is possible since the training effect weakens the exchange bias and consequently the superconducting properties of the complete hybrid.

Since we ascribe the magnetoresistance peaks mainly to the out-of-plane rotation of the magnetization the training effect that is observed in the $V(H)$ curves presented in Figs.19(b)-19(c) should also be reflected in the transverse magnetic component. Indeed, Figs. 20(a)-20(b) show detailed results for both the longitudinal and transverse components for another BL that exhibits slightly higher coercive and exchange bias fields. Panel

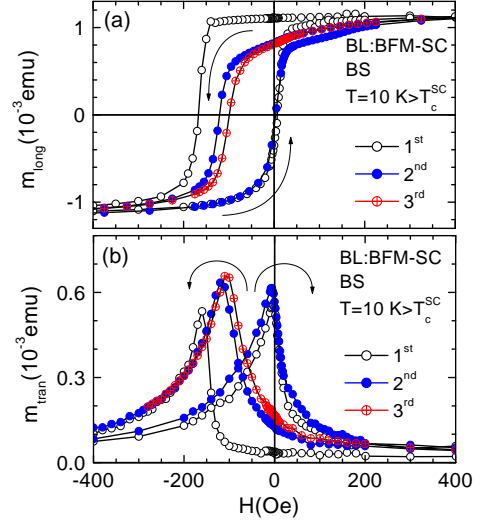


FIG. 20: (Colour online) Three successive magnetization loops for the longitudinal (a) and transverse (b) components obtained at temperature $T = 10$ K $> T_c^{SC}$ in a second BFM-SC BL that exhibits both higher coercive and exchange bias fields. All the data were obtained during a single run while the BFM-SC hybrid was BS only once, prior to the first loop.

(a) shows three successive loops for the longitudinal component, while panel (b) presents the respective data for the transverse one. Once again we stress that in these measurements the BL was exchange biased by cooling it above its blocking temperature $T_B = 100$ K under the presence of a positive magnetic field only once, prior to the very first measurement. A number of notes may be drawn from these data. First, we clearly see that the first loop (open circles) of the longitudinal [transverse] component is significantly asymmetric with the decreasing branch exhibiting a sharp downfall [rise] at 150 Oe. Second, the first loop of the longitudinal component is more square-like in comparison to the two subsequent ones. Third, the maximum value of the transverse component increases progressively with the number of performed loops. Fourth, both the coercive and exchange bias fields decrease as the number of loops progressively increases. More importantly, the decrease of these two parameters (coercive and exchange bias fields) is abrupt during the first two loops, while the third subsequent loop has only a minor effect. For instance, the full width is $W = 170$ Oe for the first round, while it gets $W = 120$ Oe and $W = 100$ Oe in the second and third rounds, respectively. This behavior is very similar to the one obtained by Dieny and colleagues⁵⁷ in NiFe/[Pt-Co] soft/hard exchange coupled BLs where it was observed that the reduction of the longitudinal component loop's width is particularly steep during the first three rounds.⁵⁷ Here, we reveal that the same behavior also holds for the transverse magnetic component. All these facts are direct consequences of the training effect: *under subsequent loops the initially induced exchange bias is weakened so that*

the in-plane magnetic order can't be maintained and the out-of-plane magnetic component progressively increases. These facts are also imprinted on the magnetoresistance curves presented in Figs.19(b)-19(c). We clearly see that the morphology of the transverse component's $m_{tran}(H)$ curves presented in Fig.20(b) is identical to the one of the magnetoresistance $V(H)$ curves shown in Fig.19(b). The training effect that is presented here for the BLs was also observed for the TLs.

Once again, we underline that although in the BLs it is also the transverse magnetic component that attains significantly high values near coercivity the observed magnetoresistance peaks are only minor when compared to the ones observed in the TLs. This is why we believe that the underlying mechanism motivating the TLs' extreme magnetoresistance peaks is the magnetic coupling of the outer FM layers through the emergence of magnetic domains and the accompanying stray fields that occur near coercivity.^{4,45,47} In the BLs the single BFM layer doesn't have this opportunity; owing to the absence of a second layer a complete stray-fields magnetostatic coupling can't be accomplished.

V. SUMMARY AND CONCLUSIONS

Summarizing, in this work we studied in detail the magnetic and transport properties of exchange biased TLs and BLs that constitute of low spin polarized $Ni_{80}Fe_{20}$ and low- T_c Nb when the external magnetic field was applied parallel to the specimens. We observed the following experimental facts:

(i) The mechanism of exchange bias may relatively promote superconductivity. This is revealed by a clear positive shift of the isothermal $V(H)$ and isofield $V(T)$ curves when the hybrids are exchange biased. In addition, the presented I-V characteristics prove that the current-carrying capability of the hybrids is significantly improved when they are exchange biased.

(ii) The fingerprints of exchange bias, that is the unidirectional anisotropy that results in a shift in the magnetization loops and the training effect that relates to weakening of the mechanism upon performing sequential loops are clearly reflected in the magnetoresistance curves that are obtained in the *superconducting* state.

(iii) The observed magnetoresistance peaks are major for the BFM-SC-PFM TLs $[(R_{max} - R_{min})/R_{nor} \times 100\% = 50\%]$, but are only minor for the BFM-SC BLs $[(R_{max} - R_{min})/R_{nor} \times 100\% = 5\%]$. We ascribe this important difference to the fact that the underlying mechanism motivating this effect in the TLs is the magnetic coupling of the outer FM layers through stray fields as the out-of-plane rotation of their magnetizations takes place near coercivity. These stray fields may exceed, primarily the SC's lower critical field, or, secondarily its upper one. In the first case the dissipation is motivated owing to flow of vortices under the driving Lorentz force that is exerted by the applied transport current, while in the sec-

ond case the normal areas that are *locally* formed should contribute extra dissipation. Although in the BLs the out-of-plane rotation of the single BFM layer's magnetization also takes place the opportunity of intense stray-fields coupling is not available due to the lack of a second FM layer so that the magnetoresistance effect is only minor.

(iv) Since the exchange bias controls the in-plane magnetic order it also controls the out-of-plane rotation and the related stray-fields magnetic coupling of the outer FM layers in the TLs. Thus, by means of exchange bias the current-carrying capability of a TL "spin valve" (see Fig.13) could be tailored at will. However, we should stress that in such "spin valves" the underlying "valving mechanism" doesn't rely on the sophisticated spin-dependent filtering process that was theoretically proposed in Refs.16,17 but on more conventional pair-breaking mechanisms. Thus, in our case such a TL should be rather called "supercurrent switch". Practical convenience is readily realizable since such devices could switch between the normal and superconducting states under the application of exchange bias on the outer FM electrodes.

(v) Going a step farther we propose that a generic prerequisite for the occurrence of extended and intense magnetoresistance peaks in a FM-SC-FM TL is that the outer FM layers should have almost the same coercive fields. When this condition is fulfilled these layers are susceptible to magnetic coupling since magnetic domains will occur simultaneously in their whole surface. Consequently, the accompanying stray fields that naturally emerge above domain walls will accomplish the magnetic coupling. Since in our TLs the one FM layer incorporates the mechanism of exchange bias its coercive field is tunable, while the respective coercivity of the other layer is fixed. Thus, by tuning the coercive field of the one FM layer we may satisfy the prerequisite of equal coercive fields for the occurrence of broad and intense magnetoresistance peaks.

The observations discussed right above may have a direct impact on the interpretations made in recent works that have dealt with relevant topics.

(i) The data presented in Figs. 19(a)-19(c) and 20(a)-20(b) are important when recent experiments that were performed in exchange biased FM-SC-FM TLs are considered (see Refs.8,9,10,11,46). Such experiments should follow a strict experimental protocol. For instance, consider the case when successive isothermal magnetoresistance $V(H)$ curves are measured as function of magnetic field at different temperatures in a TL that was exchange biased only once, prior to the first measurement. Although the original intention was to get information on the magnetic field dependence of the TL's transport behavior when this was exchange biased in every case, due to the training effect the only reliable information refers to the isothermal magnetoresistance $V(H)$ curve that is obtained during the first round of the experiment. All the subsequent ones provide an *underestimation* of the

TL's current-carrying capability since the training effect weakens significantly the exchange bias that was imposed originally prior to the very first measurement. Thus, experimental works where the exchange bias has been employed should be reconsidered under the light of these characteristics. Strict experimental protocols should always be used when the transport behavior of such exchange biased TLs and BLs is studied otherwise their properties may be underestimated.

(ii) All experimental works that treat FM-SC-FM TLs, whether these are plain or exchange biased (see Refs.8,9,10,11,12,13,14,15,44,46) and are considered as exact realizations of the theoretical propositions that refer to the "spin valve" concept (see Refs.16,17) should be reexamined under the light of the results presented in this work for exchange biased TLs and of those presented in Ref.45 for plain ones. Probably, in all cases an out-of-plane rotation and subsequent stray-fields induced magnetic coupling of the outer FM layers could be involved so that their in-plane relative magnetic configuration is not the dominant mechanism that motivates the observed effects. If this is true the theoretical propositions made in Refs.16,17 still wait for experimental evidence.

(iii) Except for results obtained in TLs also the ones that refer to more simple FM-SC BLs, whether they are plain or exchange biased (see Refs.44,46,50) should be treated more thoroughly. As it was clearly shown

in this work for exchange biased BLs and in Ref.45 for plain ones even in such simple structures the out-of-plane rotation of the FM layer's magnetization could motivate a minor magnetoresistance effect and falsify the obtained experimental results. For instance, in Ref.50 plain NiFe-Nb BLs were studied by transport measurements. The increase that was observed⁵⁰ in the magnetoresistance curves prior to the clear dips that were ascribed to the formation of "domain wall superconductivity"^{22,37,50} could be related to a partial out-of-plane rotation of the NiFe layer's magnetization.

Finally, our data show clearly that the mechanisms of exchange bias and superconductivity, that generally are considered so fundamentally different under specific circumstances may even become cooperative. In our work we used only a phenomenological basis of the involved phenomena in order to give consistent explanations for our experimental results. We hope that our experimental work not only will shed light on the contradictions that have been reported in the recent literature but will eventually trigger new experimental and theoretical work that will deal with the microscopic implications in these topics. Apart from their importance for basic physics our results could also assist the design of practical devices where the current-carrying capability of a FM-SC hybrid could be efficiently controlled by the exchange bias mechanism.

* Author to whom correspondence should be addressed; electronic address: densta@ims.demokritos.gr

- ¹ D.J. Monsma, J.C. Lodder, Th.J.A. Popma, and B. Dieny, *Phys. Rev. Lett.* **74**, 5260 (1995).
- ² B. Dieny, J. Magn. Magn. Mater. **136**, 335 (1994).
- ³ M.N. Baibich, J.M. Broto, A. Fert, F. Nguyen Van Dau, F. Petro, P. Eitenne, G. Creuzet, A. Friederich, and J. Chazelas, *Phys. Rev. Lett.* **61**, 2472 (1988).
- ⁴ S. Gider, B.-U. Runge, A.C. Marley, and S.S.P. Parkin, *Science* **281**, 797 (1998).
- ⁵ J. Mathon, and A. Umerski, *Phys. Rev. B* **63**, 220403 (2001).
- ⁶ S. Yuasa, T. Nagahama, A. Fukushima, Y. Suzuki, and K. Ando, *Nat. Mater.* **3**, 868 (2004).
- ⁷ D.D. Djayaprawira, K. Tsunekawa, M. Nagai, H. Maehara, S. Yamagata, N. Watanabe, S. Yuasa, Y. Suzuki, and K. Ando, *Appl. Phys. Lett.* **86**, 092502 (2005).
- ⁸ J.Y. Gu, C.-Y. You, J.S. Jiang, J. Pearson, Ya.B. Bazaliy, and S.D. Bader, *Phys. Rev. Lett.* **89**, 267001 (2002).
- ⁹ A. Potenza and C.H. Marrows, *Phys. Rev. B* **71**, 180503(R) (2005).
- ¹⁰ I.C. Moraru, W.P. Pratt, Jr., and N.O. Birge, *Phys. Rev. Lett.* **96**, 037004 (2006).
- ¹¹ I.C. Moraru, W.P. Pratt, Jr., and N.O. Birge, *Phys. Rev. B* **74**, 220507(R) (2006).
- ¹² V. Peña, Z. Sefrioui, D. Arias, C. Leon, J. Santamaria, J.L. Martinez, S.G.E. te Velthuis, and A. Hoffmann, *Phys. Rev. Lett.* **94**, 57002 (2005).
- ¹³ A.Yu. Rusanov, S. Habraken, and J. Aarts, *Phys. Rev. B* **73**, 060505(R) (2006).

- ¹⁴ C. Visani, V. Peña, J. Garcia-Barriocanal, D. Arias, Z. Sefrioui, C. Leon, J. Santamaria, N.M. Nemes, M. Garcia-Hernandez, J.L. Martinez, S.G.E. te Velthuis, and A. Hoffmann, *Phys. Rev. B* **75**, 054501 (2007).
- ¹⁵ A. Singh, C. Sürgers, and H.v. Löhneysen, *Phys. Rev. B* **75**, 024513 (2007).
- ¹⁶ A.I. Buzdin, A.V. Vedyayev, and N.V. Ryzhanova, *Europhys. Lett.* **48**, 686 (1999).
- ¹⁷ L.R. Tagirov, *Phys. Rev. Lett.* **83**, 2058 (1999).
- ¹⁸ T. Lfwander, T. Champel, J. Durst, and M. Eschrig, *Phys. Rev. Lett.* **95**, 187003 (2005).
- ¹⁹ B. Jin, J. Magn. Magn. Mater. (2007), doi:10.1016/j.jmmm.2007.01.001
- ²⁰ D. Stamopoulos, N. Moutis, M. Pissas, and D. Niarchos, *Phys. Rev. B* **72**, 212514 (2005).
- ²¹ D. Stamopoulos, *Supercond. Sci. Technol.* **19**, 652 (2006).
- ²² D. Stamopoulos and M. Pissas, *Phys. Rev. B* **73**, 132502 (2006).
- ²³ A.F. Volkov, F.S. Bergeret, and K.B. Efetov, *Phys. Rev. Lett.* **90**, 117006 (2003).
- ²⁴ F.S. Bergeret, A.F. Volkov, and K.B. Efetov, *Phys. Rev. Lett.* **86**, 4096 (2001).
- ²⁵ F.S. Bergeret, A.F. Volkov, and K.B. Efetov, *Phys. Rev. B* **69**, 174504 (2004).
- ²⁶ M. Eschrig, J. Kopu, J.C. Cuevas, and G. Schön, *Phys. Rev. Lett.* **90**, 137003 (2003).
- ²⁷ M. Eschrig, T. Löfwander, T. Champel, J.C. Cuevas, J. Kopu, and G. Schön, *J. Low Temp. Phys.* (2007), doi:10.1007/s10909-007-9329-6
- ²⁸ Ya.V. Fominov, A.F. Volkov, and K.B. Efetov,

- cond-mat/0610440 (2006).
- 29 K.B. Efetov, I.A. Garifullin, A.F. Volkov, and K. Westerholt, cond-mat/0610708 (2006).
 - 30 A.I. Buzdin, L.N. Bulaevskii, and S.V. Panyukov, Sov. Phys. JETP **60**, 174 (1984).
 - 31 A.I. Buzdin, and A.S. Melnikov, Phys. Rev. B **67** 020503(R) (2003).
 - 32 A.Yu. Aladyshkin, A.I. Buzdin, A.A. Fraerman, A.S. Mel'nikov, D.A. Ryzhov, and A.V. Sokolov, Phys. Rev. B **68** 184508 (2003).
 - 33 T. Champel, and M. Eschrig, Phys. Rev. B **71**, 187003(R) (2005); *ibid.*, **72**, 054523 (2005).
 - 34 T. Lfwander, T. Champel, and M. Eschrig, Phys. Rev. B **75**, 014512 (2007).
 - 35 M.A. Maleki and M. Zareyan, Phys. Rev. B **74**, 144512 (2006).
 - 36 A.I. Buzdin, Rev. Mod. Phys. **77**, 935 (2005).
 - 37 M. Houzet and A.I. Buzdin, Phys. Rev. B **74**, 214507 (2006).
 - 38 C. Monton, F. de la Cruz, and J. Guimpel, Phys. Rev. B **75**, 064508 (2007).
 - 39 W. Gillijns, A.Yu. Aladyshkin, M. Lange, M.J. Van Bael, and V.V. Moshchalkov, Phys. Rev. Lett. **95**, 227003 (2005).
 - 40 Z. Yang, M. Lange, A. Volodin, R. Szymczak, and V.V. Moshchalkov, Nature **3**, 793 (2004).
 - 41 J. Fritzsche, V.V. Moshchalkov, H. Eitel, D. Koelle, R. Kleiner, and R. Szymczak, Phys. Rev. Lett. **96**, 247003 (2006).
 - 42 V.V. Ryazanov, V.A. Oboznov, A.S. Prokofiev, and S.V. Dubonos, Pis'ma Zh. Eksp. Teor. Fiz. **77**, 43 (2003) [JETP Lett. **77**, 39 (2003)].
 - 43 C. Bell, S. Tursucu, and J. Aarts, Phys. Rev. B **74**, 214520 (2006).
 - 44 R. Steiner and P. Ziemann, Phys. Rev. B **74**, 094504 (2006).
 - 45 D. Stamopoulos, E. Manios, and M. Pissas, Phys. Rev. B **75**, 184504 (2007).
 - 46 D. Stamopoulos, E. Manios, and M. Pissas, Phys. Rev. B **75**, 014501 (2007).
 - 47 L. Thomas, M.G. Samant, and S.P. Parkin, Phys. Rev. Lett. **84**, 1816 (2000).
 - 48 L. Neel, C. R. Acad. Sci. **255**, 1676 (1962).
 - 49 S. Demokritov, E. Tsybal, P. Grunberg, W. Zinn, and I.K. Schuller, Phys. Rev. B **49**, 720 (1994).
 - 50 A.Yu. Rusanov, S. Habraken, J. Aarts, and A.I. Buzdin, Phys. Rev. Lett. **93**, 057002 (2005).
 - 51 D. Stamopoulos, M. Pissas, and E. Manios, Phys. Rev. B **71**, 014522 (2005).
 - 52 W.H. Meiklejohn and C.P. Bean, Phys. Rev. **105**, 904 (1957).
 - 53 J. Nogues, and I. K. Schuller, J. Magn. Magn. Mater. **192**, 203 (1999).
 - 54 A.E. Berkowitz, and K. Takano, J. Magn. Magn. Mater. **200**, 552 (1999).
 - 55 M. Gruyters, and D. Riegel, Phys. Rev. B **63**, 052401 (2000).
 - 56 E.E. Fullerton, J.S. Jiang, M. Grimsditch, C.H. Sowers, and S.D. Bader, Phys. Rev. B **58**, 12193 (1998).
 - 57 J. Sort, A. Popa, B. Rodmacq, and B. Dieny, Phys. Rev. B **70**, 174431 (2004).
 - 58 S. Mangin, T. Hauet, Y. Henry, F. Montaigne, and E.E. Fullerton, Phys. Rev. B **74**, 024414 (2006).
 - 59 E.E. Fullerton, J.S. Jiang, and S.D. Bader, J. Magn. Magn. Mater. **200**, 392 (1999).
 - 60 C.L. Chien, V.S. Gornakov, V.I. Nikitenko, A. J. Shapiro, and R.D. Shull, Phys. Rev. B **68**, 014418 (2003).
 - 61 M. Ali, P. Adie, C.H. Marrows, D. Greig, B.J. Hickey, and R.L. Stamps, Nature Materials **6**, 70 (2007).
 - 62 A.E. Berkowitz, J.R. Mitchell, M.J. Carey, A.P. Young, S. Zhang, F.E. Spada, F.T. Parker, A. Hutten, and G. Thomas, Phys. Rev. Lett. **68**, 3745 (1992).
 - 63 J.Q. Xiao, J.S. Jian, and C.L. Chien, Phys. Rev. Lett. **68**, 3749 (1992).
 - 64 D. Stamopoulos, E. Manios, and M. Pissas, submitted for publication.
 - 65 T.W. Clinton, and M. Johnson, Appl. Phys. Lett. **76**, 2116 (2000); *ibid.*, J. Appl. Phys. **85**, 1637 (1999).